People's Democratic Republic of Algeria
Ministry of Higher Education and Scientific Research

University M'Hamed BOUGARA – Boumerdès

Institute of Electrical and Electronic Engineering

Department of Control and Power Engineering

Project Report Presented in Partial Fulfilment of

the Requirements of the Degree of

'MASTER'

In Control Engineering

Title:

Integrated Microgrid Protective System using PMU

Presented By:

- **NEGGAZ Taima**

Supervisor:

Dr.A.OUADI

2021/2022

Abstract

With the penetration of microgrids in power systems, conventional protections have become inefficient due to the resulted changes in current characteristics and power flow direction. Therefore microgrids have to incorporate smart protection systems. The integrated MG protective system developed in this project is based on phasor measurement unit data measurements of current and voltage. This protection can detect and isolate 3 phase short circuit faults as well as abnormalities such as overload, overvoltage and undervoltage in the different buses of the MG.

Acknowledgment

Praise to God, the supreme for leading me during all these years of my study path, and for giving me the courage and strength to accomplish this project successfully despite all the difficulties, Alhamdulilah.

I would like to express my deepest and sincere gratitude to my teacher and supervisor **Prof. OUADI Abderrahmane** for his invaluable patience and feedback and who followed this project with great interest and guided me throughout this journey . I deeply appreciate his precious advice and sincerity that helped me to fulfill this work.

Additionally, I am extremely grateful to **Prof.BENTARZI Abdelhamid** for his precious advice time and instructions that made the accomplishment of this project possible.

I sincerely thank the jury members who generously provided knowledge and expertise and for taking time to read and analyse this project report.

Dedication

To my parents for their endless love, support and encouragement throughout my pursuit for education. I hope this achievement will fulfill the dream they envisioned for me,

To my beloved sisters Oussoua, Tasnime & Belssem for their trust and support,

To my besties Kenza and Assia for their encouragement and being always by my side.

To my soulmate Anfal for being a source of inspiration,

To all my family .

I dedicate this work to you all. May this accomplishment meet your long-held wishes and reflect your endless support.

TAIMA

Contents

List of Figures

List of Tables

List of Abbreviations and Symbols

γ_i Abnormality Coefficient

γ_i Abnormality Coefficient

D_{index} Short Circuit Index

D_{index} Short Circuit Index

DER Distributed Energy Resources

EDLC Electrochemical Double Layer Capacitor

EDS Electric Distribution System

GPS Global Position System

LV Low Voltage

MG Microgrid

MGCC Microgrid Central Controller

MV Medium Voltage

$\mathbf{O}_i$ Overcurrent

$\mathbf{O}_i$ Overcurrent

$\mathbf{O}_v$ Overvoltage

$\mathbf{O}_v$ Overvoltage

PCC Point Common Coupling

PD Protective Device

PMU Phasor Measurement Unit

PPS Pulse Per Second

PV Photovoltaic

RE Renewable Energy

RMS Root Mean Sequare

SC Short Circuit

SPS Smart Protection System

U$_v$ Undervoltage

U$_v$ Undervoltage

General Introduction

Microgrid (MG) is a smaller-scale power system version of standard grid. A smart microgrid is an electricity grid that offers more intelligent electricity generation, distribution, and flow control to local electrical consumers [1].It has two operation modes: the grid connected mode and the islanded mode.

In order to protect human being, materials and power systems; protection of MG plays an important role during both operation modes. The majority of faults occurs when the system is operating in the islanded mode[2].

Conventional protections like differential and overcurrent protections can not be operated in all type of faults since they will suffer from sensitivity issues and reduce the reliability of the operating system[3].Thus, a smart adaptive protection is needed in such systems in order to insure its functionality, enhance its reliability and avoid blackouts. The smart protection must have synchronized data and time tagged measurements to have the ability of avoiding overlapping problems as well as the bidirectional power flow issues since traditional protections are used for detecting faults in unidirectional power systems.

This project proposes an adaptive smart protection system (SPS) which is able to operate in both grid-connected mode and islanded mode in order to detect 3ϕ short circuit (SC) faults and abnormalities. This protection is based on µPMU device to provide synchronized phasors with high accuracy and speed to a central phasor data concentrator and a smart global MG protective system.

Many other primary and backup protective functions can be included, as differential protection, bidirectional over current protection functions, etc.

The first chapter is an introduction to the MG and its characteristics and components in addition to its different types and operating modes.

The µPMU is introduced in the second chapter in addition to phasors and synchrophasors with all their equations and calculations methods.

The proposed SPS algorithm is defined in chapter three with all its necessary techniques of calculations and transformations. This chapter also presents a power system model in order to test the SPS in addition to some 3 µPMU measurements.

The last chapter includes the protection block diagram and the test scenario of faults where the SPS was applied to fault detection and isolation of the MG power network. The obtained results from this simulation are discussed.

Chapter 1

Introduction to Microgrid

1.1 Introduction

In the next few decades, the fossil fuel material will disappear by cause of their massive usage in producing energy that require a renovation of energy resources. An effective and efficient solution for this issue is going toward renewable resources such as wind, hydraulic and solar energies.

Smart MG is a practical process to integrate renewable energy (RE) in power systems, Furthermore, it allows the participation of the community by permitting customers taking part in the electrical business. This contributes to the Perfect Power System's foundation.

This chapter introduces the smart grid types and their components as well as the major problems and issues of power systems during the connection to the MG and when it is disconnected.

1.2 Microgrid History

When Thomas Edison opened his Pearl Street Station in 1882, there was no standard for a generation-distribution system for electricity, so he built his own station. Edison's Manhattan Pearl Street Station, astonishingly, met all of today's standards for a MG system. It was self-contained, with six giant generators driven by coal-fired steam engines. His generators each put out 1,100 kW of DC power**http**. In the late 1990s, the term 'microgrid' appears when the US Department of Energy (USDOE) began initiatives to investigate grid dependability and how to maximize the use of dispersed generating resources to improve reliability and resiliency at the request of the US Congress[4].

1.3 Definitions of Microgrid

The majority of MG definitions lead to the same meaning is that a MG is a local network produces electricity from different energy resources, this electricity will be distributed and consumed through the loads of the network, it may operate in two modes standalone mode and grid-connected mode.

The US department of energy defines the MG as "a group of interconnected loads and distributed energy resources within clearly defined electrical boundaries that acts as a single controllable entity with respect to the grid. A microgrid can connect and disconnect from the grid to enable it to operate in both grid-connected or island mode" .

According to IEEE standard (CPE.2018.8372506) " Microgrids are localized grids that can disconnect from the traditional grid to operate autonomously. Because they are able to operate while the main grid is down, microgrids can strengthen grid resilience and help mitigate grid disturbances as well as function as a grid resource for faster system response and recovery" .

Microgrid Institute: "A microgrid is a small energy system capable of balancing captive supply and demand resources to maintain stable service within a defined boundary. There's no universally accepted minimum or maximum size for a microgrid" [5].

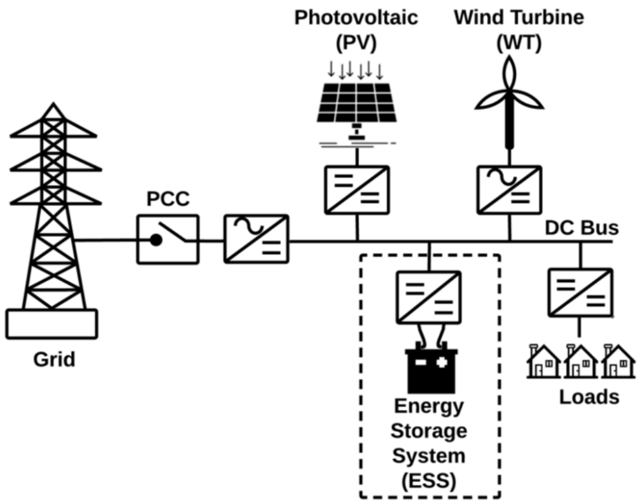

Figure 1.1: Typical topology of microgrid [6]

1.4 Characteristics of Microgrid

MG has different characteristics which are listed below [7]:

- **Independence:** " MG can operate in islanded mode. In autonomous operation, MG is capable of balancing generation and load. Besides, It can keep system voltage and frequency in defined limits with adequate controls."
- **Flexibility:**" The expansion and growth rate of MGs do not need to follow any precise forecasts. According to operation modes, MGs can operate in different modes. Connecting to the main grid is optional."
- **Stability:** "MG can operate stably during nominal operating modes and transient events, no matter whether the larger grid is up or down"
- **Interactivity:** "MGs are compatible with the main grid. They can support the main grid if it is necessary and the main grid can also supply for MGs."
- **Expanse:** "MGs can grow easily by adding more DERs and loads. It is easier than expand the traditional grid."
- **Efficiency:** "The utilization of DERs optimization and manage loads by using centralized as well as distributed MG controller is the way to make energy management goals optimization."
- **Economic:**"The utilization of DERs is the key to reduce fuel cost and CO2 emissions".

1.5 Microgrid Components

MG system consists of three subsystems: a distributed generation (DG) unit , an energy storage system (ESS) and loads. The mentioned subsystems are supervised by the MG controller as explained in Fig 1.2

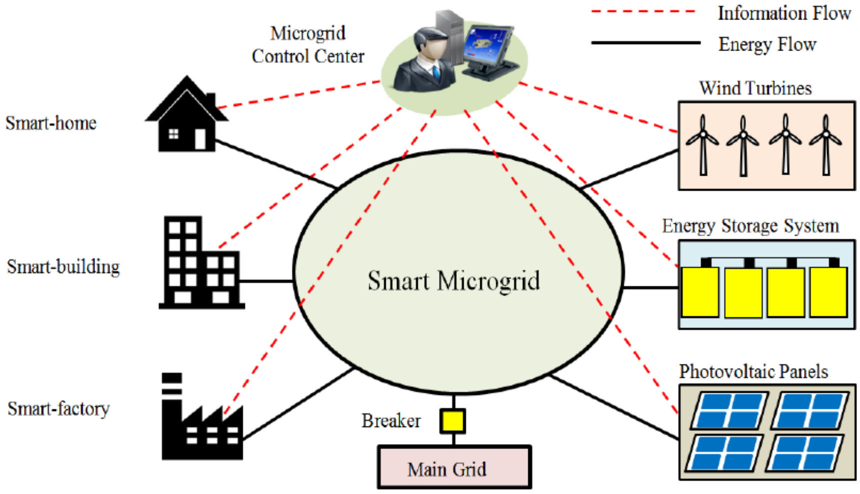

Figure 1.2: Components of microgrid [8]

1.5.1 Distributed Generation Unit

DG units are mainly composed of RE sources. The use of these sources in power systems is increasing every year because of their availability, sustainability, ease of use and connection with the MG, cheap cost, and environmental impact. The lack of fossil fuels and the simplicity of maintaining RE sources increase people's reliance on them and their desire to build energy farms [9].

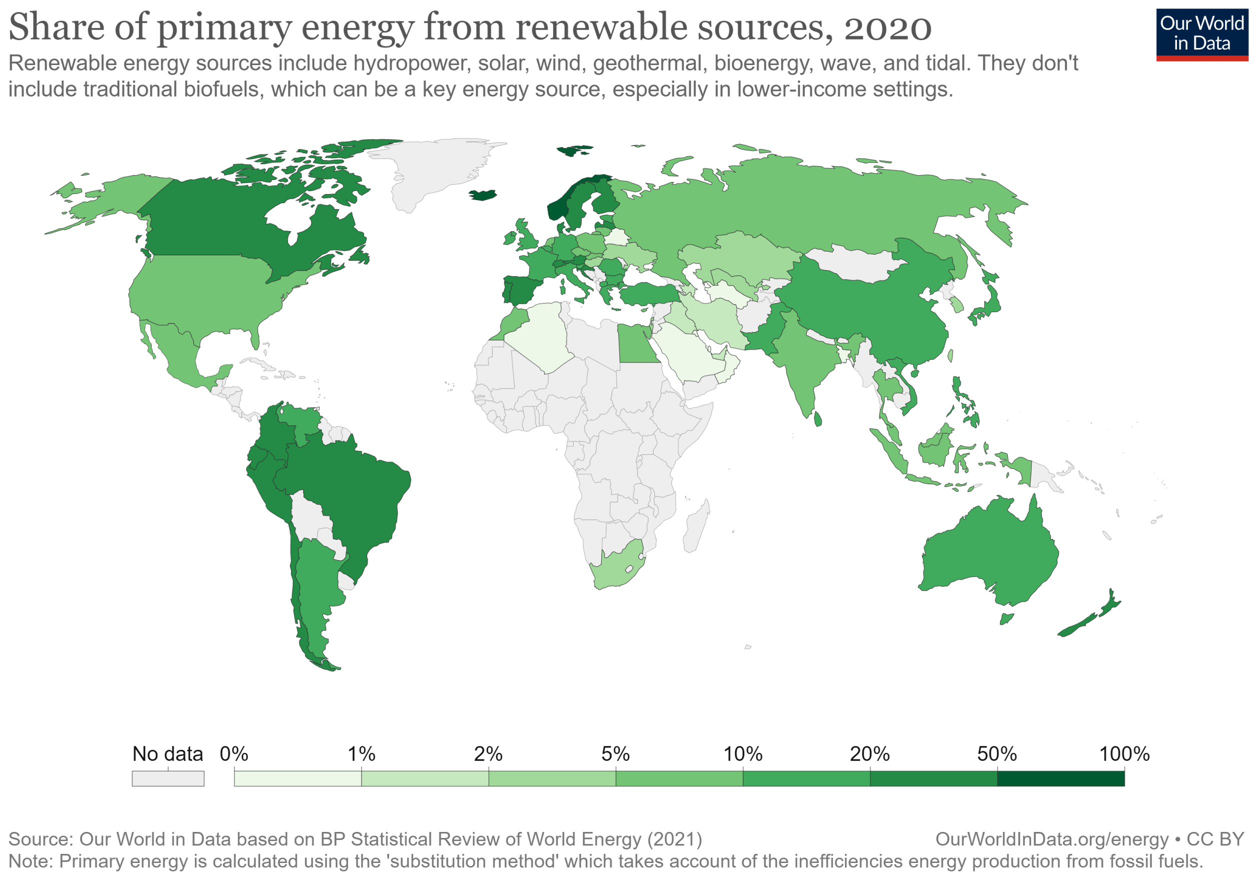

Figure 1.3: Renewable energy sources around the world [10]

1.5.2 Energy Storage System

RE sources are not stable due to the weather changes which affects the MG negatively [11]. A hybrid energy storage system of super-capacitor, battery and flyweel is used to compensate the system due to their fast energy absorption and a long-term storage ability.

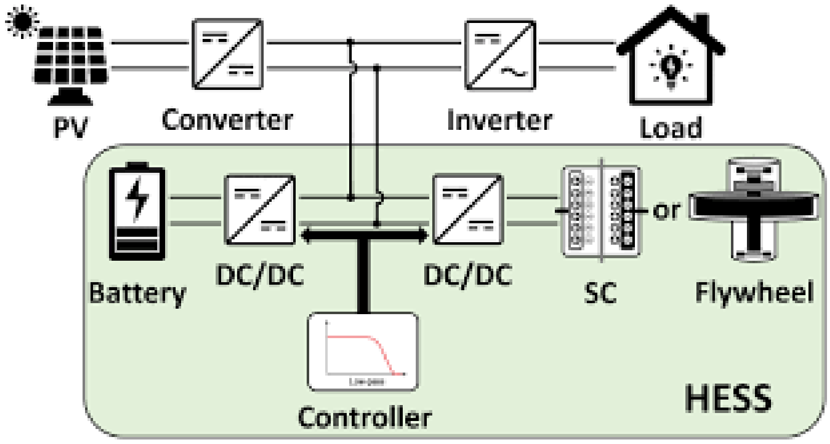

Figure 1.4: MG with hybrid energy storage system[12]

- **Super-capacitor**

Super-capacitor is an electrochemical double layer capacitor (EDLC) that stores electric energy in both electrostatic and electrochemical energy storage forms using the double layer. Its power density is 10-100 times that of ordinary batteries, making it suitable for short-term high power output [13].

a Equivalent model of super-capacitor

b Commercial super-capacitor[14]

Figure 1.5: Super-capacitor storage device

- **Battery**

Battery is an electrochemical storage device. The main types of batteries used in MG are lead-acid, lithium-ion, zinc-bromine, Tesla Powerwall, sodium nickel cadmium[15]. It is used for long-term high power storage.

a Tesla Powerwall Battery [16]

b zinc bromine battery [17]

c Lead-acid battery[18]

d Lithium-ion battery[19]

Figure 1.6: Different battery types

- **Flywheel**

Flywheel is an mechanical storage device, it is used before the chemical storage devices, its logic of working is a rotating mass stores rotatable energy and when energy is required the rotating mass is linking with the generator[1].

Figure 1.7: Flywheel energy storage [20]

1.5.3 Loads

Loads are the last stage where the produced energy will be consumed, there are two types of loads DC and AC. On the other hand loads can be divided into three categories:

- **Sensitive loads**

They are the most important loads in the MG for the reason that it is highly requested to never be dropped whatever the situation of the MG like hospitals and nursing facilities[21].

- **Non-sensitive loads**

These loads can be dropped for a short period of time or time shifted, these are loads that can be reduced to allow further generation to begin like heating, ventilating and air-conditioning...[21].

- **Emergency loads**

They are the only kind of loads that should be thrown away in an emergency to keep the MG stable and avoid a blackout like residential users, commercial establishments with backup generators[21].

1.6 Microgrid Types

The type of MG depends on the type of the loads so we can derive the following types :

1.6.1 DC Microgrid

The majority of DG units of DC MGs are composed of PV solar generators since they generate DC power in addition to the availability of solar energy . DC MGs are an excellent choice if the loads of the MG are building's lights (LEDs), phone's chargers... [5].The main advantage of DC MGs is the reduction of power quality issues such as reactive power and harmonics in addition to power converters which raises costs and reduces reliability due to converter outages[22].

1.6.2 AC Microgrid

AC MGs are too similar to traditional grids, the only difference is that they are powered and controlled locally, also they feed local loads. AC MGs are connected to power sources through AC-DC converters because the majority of this sources are DC and that limit the use of this type of networks [5]. The main advantage of AC MGs is their high reliability and their main disadvantages are problems of synchronization and power quality [22].

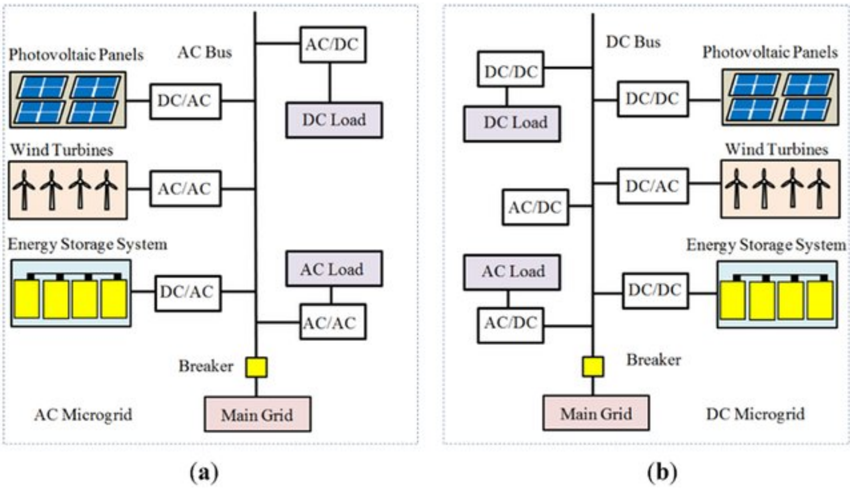

Figure 1.8: (a) AC microgrid ,(b) DC microgrids [23]

1.6.3 AC/DC Microgrid

Hybrid or AC/DC MGs is a combination between the two previous types therefore power losses are reduced as result of minimization of converters. This type has the least possible cost and the best performance [5][22].

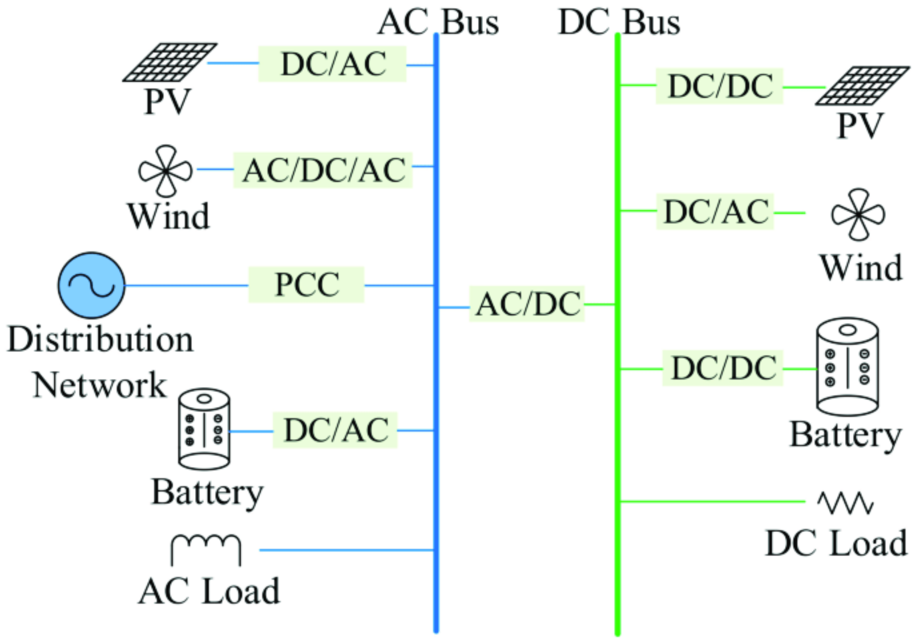

Figure 1.9: Hybrid microgrid[24]

1.7 Microgrid Operation Modes

One of the interesting feature of MG is that it can operate in the both situations, when it is connected to the main grid (grid-connected mode) and when it is disconnected from it (islanded mode).

1.7.1 Grid-connected Mode

Grid-connected mode means that the MG is connected to the main grid and follows its distribution rules and for stability reasons the MG can not impose its control decisions in this mode.The MG can either draw power from or supply power to the main grid, then it functions as a regulated load or a source[25].

1.7.2 Islanded Mode

MG is said to be in islanded mode when it is disconnected from the grid at the point of Common Coupling (PCC) and operates as a standalone system. The MG switch to this mode if unexpected event appears in the grid such as faults and storms, or it may be planned due to maintenance issues. In this mode the MG works under the decisions of its own controller [26].

1.8 Microgrid and Protection

Protection system methods have become increasingly important as the complexity and challenges in power systems have grown. The basic purpose of a protection system is to keep the fault component separate from the healthy section in order to provide a steady supply of electrical energy free of interruptions, hence avoiding cascading failures, and blackouts.

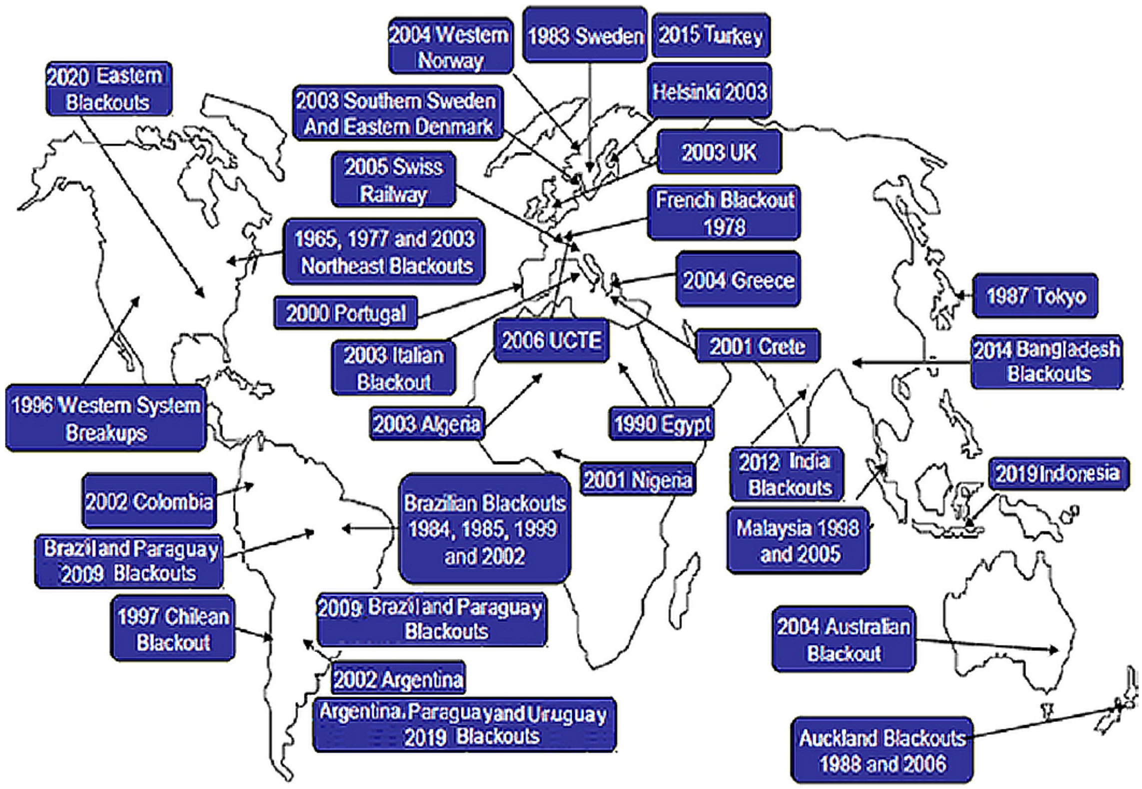

Figure 1.10: History of worldwide blackouts and disturbances [27]

1.8.1 Blackouts Around the World

A blackout occurs when the electrical grid is completely shut down due to an imbalance in power generation and consumption.

A blackout struck India's north and east on July 30, 2012, lasting roughly 15 hours and affecting nearly 620 million people. The blackout was caused by overloading on one of the 400 kV Gwali–Binar transmission lines while the other line was disconnected for maintenance. A demand-generation imbalance caused the system to fail again the next day, affecting 700 million people and disrupting nearly 32 GW of energy. In terms of the number of people affected, this blackout is the most extensive power outage ever recorded[28].

Table 1.1: Number of power outages recorded in different parts of the world in 2011.

Region	Number of Power Outages	Duration of Each Power Outage (hours)
East Asia and Pacific	200	6.00
Eastern Europe and Central Asia	100	6.50
Latin America and Caribbean	40	8.00
Middle East & North Africa	50	4.00
South Asia	1200	2.50
Sub Saharan Africa	210	7.50
The rest of the countries	250	5.00

1.8.2 Blackouts Causes

The table below summarize 66 major power system blackouts were evaluated in various parts of the world from 2011 to 2019 . Although the study does not include all power outages around the world but it is a useful tool for analysing the causes of power outages. The majority of blackouts were caused by unusual meteorological conditions such as intense winds and large storms, as well as trees falling on power lines[28].

Table 1.2: Analysis on blackouts around the world and their percentage from 2011 to 2019

Blackout Cause	Number Recorded	% of the Recorded Number
Weather/Trees	33	50
Faulty equipment or human error	21	31.8
Vehicle/Accidents	7	10.6
Animals	1	1.5
Over demand	4	6.1
Total	66	100

1.9 Conclusion

In conclusion, it is evident that MGs are the future of power systems since they have renewable sources of energy and efficient storage system. In addition, their different operation modes as stand-alone system or as a part of the main grid along with their ability of feeding the different loads and in some cases supporting the main grid.

On the other hand, MGs still need efficient protection systems to avoid blackouts and improve their performance.

Chapter 2

Phasor Measurement Unit Overview

2.1 Introduction

The smart grid is the perfect solution for today's energy system problems as the need of fully automated, highly efficient and self-stable energy systems grow [29].This can be performed using the PMU since it uses an advanced information technology and communication systems to provide phasor measurements with high accuracy and speed.

This chapter describes the PMU and its main hardware parts, in addition to the discrete fourier transform and the way of extracting phasors of a sinusoidal signal.

2.2 Phasor Measurement Unit

2.2.1 Definition of PMU

A PMU is a stand-alone device that provides phasor and frequency measurements by measuring AC voltage and/or current signals of 50/60Hz. For each phase, an analog to digital converter digitizes the signal, and a phase-lock oscillator and global position system (GPS) reference time source (commonly referred to pulses per second (PPS)) enable fast time synchronization. GPS is currently the only regionally synchronized signal source with sufficient accuracy for phasor measurements[30]. The PMU calculates the grid frequency, voltage, and current phasors at high sampling rates and sends the data over the networked communication line, along with the associated GPS time stamps[31].The recently developed µPMU claims to have millimeter-level precision and 100 times the resolution of a traditional transmission-type PMU. PMUs may therefore be a very useful tool for distribution networks and microgrids. [32].

2.2.2 SCADA and PMU

SCADA was commonly utilized to show and manage the power network before PMU (µPMU) began to be employed within the transmission and distribution networks. SCADA is mostly based on the steady state of the network, therefore it can't operate at the dynamic state due to unsynchronized statistics . PMU and µPMU are used to measure voltage and current in order to use the in tracking and controlling transmission network wide-location and distribution network neighborhood location[33].

Table 2.1: Comparison between SCADA and PMU

ATTRIBUTE	SCADA	PMU & FPMU
Resolution	1 sample every (2-4) sec.	(10-120) samples per sec.
Observability	Steady-state	Dynamic/Transient state
Phase angle measurement	No phase angle	Provides phase angle
Time synchronization	Measurements are not synchronized	Measurements are time-synchronized
Monitoring and control	Local	Wide-area & Local

2.3 PMU Hardware Architecture

As shown in the Fig 2.1 the PMU components can be divided in three functions: synchronization, measurement and transmission.

2.3.1 Synchronization

It is composed of a GPS receiver and a phase-locked oscillator to keep the input signal synchronized.

2.3.2 Measurement

The input signal passes through the anti-aliasing filter (low pass filter) then to the analog to digital converter in order to sample the signal before it accesses to the measurement unit which calculate the RMS value, the phase angle and the frequency of the signal.

2.3.3 Transmission

The measured data will be sent using a suitable transmission protocol.

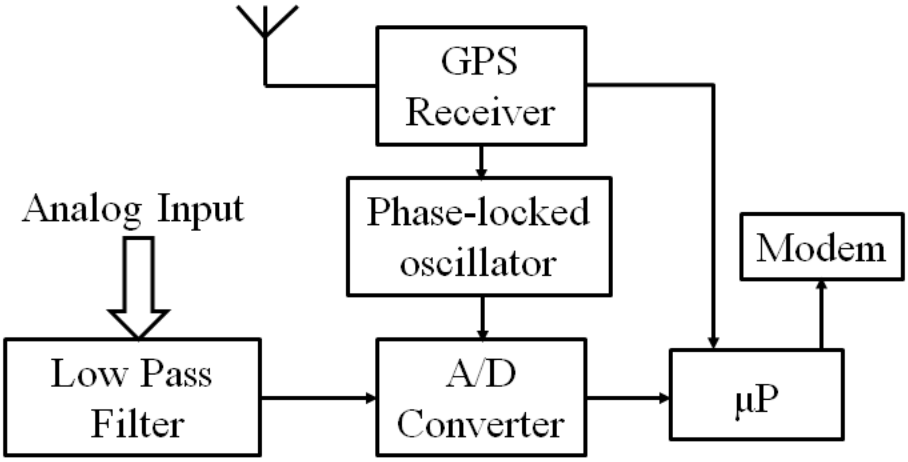

Figure 2.1: PMU architecture [31]

2.4 PMU Applications

Phasor measurements obtained by PMUs can be utilized for a variety of applications to maintain and improve power system reliability. In North America, Europe, China, and Russia, PMUs have been employed in post-disturbance analysis, stability monitoring, thermal overload monitoring, power system restoration, and model validation. PMU applications for state estimation, real-time control, adaptive protection, and wide area stabilizer are being tested or planned in these nations. India and Brazil are either planning or experimenting with the use of PMUs in their power grids[34]. Table 2.2 illustrates some PMU applications examples.

2.4.1 Control

Prior to the introduction of phasor measurements, all power system control was dependent on local data and mathematical models of the wider system. It is well known that such controllers are rarely optimal, and that when the model is inaccurate, they can provide completely inappropriate system responses. The idea of integrating phasor measurement in such systems to increase the control ability of power system elements has been investigated for several years. PMUs give a very excellent solution to the power system controller problem by providing high-speed synchronous phasor measurements[35].

2.4.2 Monitoring

A power system's operating system can be dynamically changed by severe changes in system conditions. Traditional monitoring techniques use real and reactive power injections and flows to estimate system states. Because the measurements were not synchronized across the system, the measurements at a given time had to be inferred from the obtained measurements to ascertain the states at that time. The estimator would be linear and relatively straightforward to develop because the system states are linear functions of voltage and current data. PMU readings are time synchronised and sent at a high rate with time stamps[36].

2.4.3 Protection

Fault protection is an essential when it comes to creating MG. An effective protection coordination approach isolates as minimum of the system as possible when a failure occurs, avoiding excessive power disconnection to areas that are not affected by the fault. Protection coordination, in this view, requires designing protection systems so that each protective device performs its primary function as quickly as possible while being backed up by another protective device in the event that it fails[37].

Table 2.2: PMU applications examples [34]

Topics	**Applications**	**Description**
Reliability Operations	Wide-area grid monitoring and visualization	Use phasor data to monitor and alarm for metrics across entire interconnection (frequency stability, voltage, angle differences, MW and MVAR flows).
	Power plant monitoring and integration	Use real-time data to track and integrate power plant operation (including intermittent renewables and distributed energy resources.
	Alarming for situational awareness tools	Use real-time data and analysis of system conditions to identify and alert operators to potential grid problems
	State estimation	Use actual measured system condition data in place of modeled estimates.
	Inter-area oscillation monitoring , analysis and control	Use phasor data and analysis to identify frequency oscillations and initiate damping activities.
	Automated real-time control of assets	Use phasor data and analysis to identify frequency oscillations and initiate damping activities.
	Wide-area adaptive protection and system integrity protection	Real-time phasor data allow identification of grid events and adaptive design, execution and evaluation of appropriate system protection measures
	Planned power system separation	Improve planned separation of power system into islands when instability occurs, and dynamically determine appropriate islanding boundaries for island-specific load and generation balances.
	Dynamic line ratings and VAR support Day-ahead and hour-ahead operations planning	Use PMU data to monitor or improve transmission line rating in real time. Use phasor data and improved models to understand current, hour-ahead, and day-ahead system operating conditions under a range of normal and potential contingency operating scenarios.
	Automatically manage frequency and voltage response from load system reclosing and power system restoration	System load response to voltage and frequency variations. attempts.

Market operation	Congestion analysis	Sychronized measurements make it possible to operate the grid according to true real-time dynamic limits, not conservative limits derived from off-line studies for worst-case scenarios.
Planning	Static model benchmarking, Dynamic model benchmarking	Use phase data to better understand system operations, identify errors in system modeling data, and fine-tune power system models for on-line and off- line applications (power flow, stability,short circuit, OPF, security assessment, modal frequency response, etc.). Phasor data record actual system dynamics and can be used to validate and calibrate dynamic models.
	Generator model validation Stability model validation Performance validation	Use phasor data to validate planning models, to understand observed system behavior and predict future behavior under assumed conditions.
Others	Phasor applications vision,road mapping & planning	Real-time phasor data allow identifica- tion of grid events and adaptive design, execution and evaluation of appropriate system protection measures
	Planned power system separation	Improve planned separation of power system into islands when instability occurs, and dynamically determine appropriate islanding boundaries for island-specific load and generation balances.
	Dynamic line ratings and VAR support Day-ahead and hour-ahead operations planning	Use PMU data to monitor or improve transmission line rating in real time Use phasor data and improved models to understand current, hour-ahead, and day-ahead system operating conditions under a range of normal and potential contingency operating scenarios.

2.5 Phasor Estimation Using DFT Algorithm

2.5.1 Phasors

A phasor is a complex version of a sinusoidal wave quantity where the complex angle (in polar form) is the cosine wave phase angle and the complex modulus is the cosine wave amplitude[38]. Consider the following sinusoidal signal expressed by

$$x(t) = X_m\, cos(2\pi ft + \phi) \tag{2.1}$$

Its phasor representation is presented by the following equation

$$
\begin{aligned}
X &= (X_m/\sqrt{2})\exp j\phi \\
&= (X_m/\sqrt{2})\ cos\phi + jsin\phi \\
&= X_r + jX_i
\end{aligned}
\tag{2.2}
$$

where X_m: is the peak value of the signal .

f: is the nominal frequency of the signal.

ϕ: is the phase angle of the signal.

X_r: is the real component of the signal.

X_i: is the imaginary component of the signal.

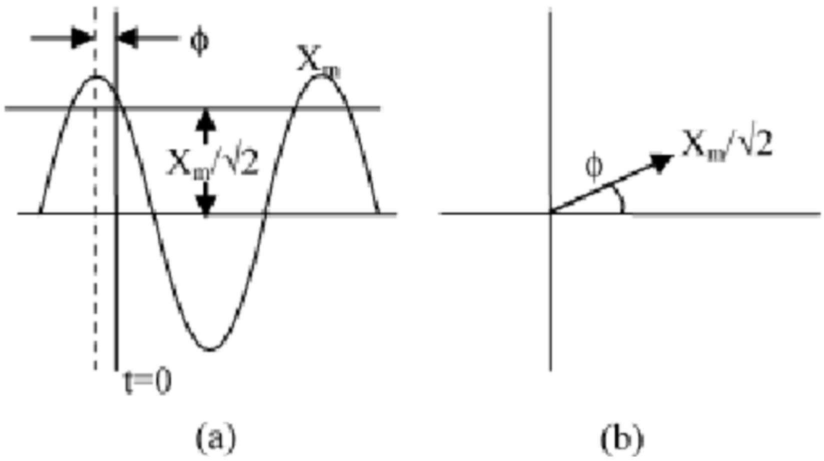

Figure 2.2: (a) sinusoidal signal, (b) its Phasor [38]

2.5.2 Synchrophasors

Asynchronized phasor or synchrophasor is a phasor generated from data samples with the measurement's reference being a standard time signal [38] In AC power system The AC power signal's amplitude and phase angle are both represented by phasors. phase angle is measured In relation to the time of measurement, A synchronizing source must provide a common time reference in order to compare the measured phasors throughout an interconnected grid. As long as it supplies all of the sites in the comparison zone, the synchronizing source can be local or global. [30].

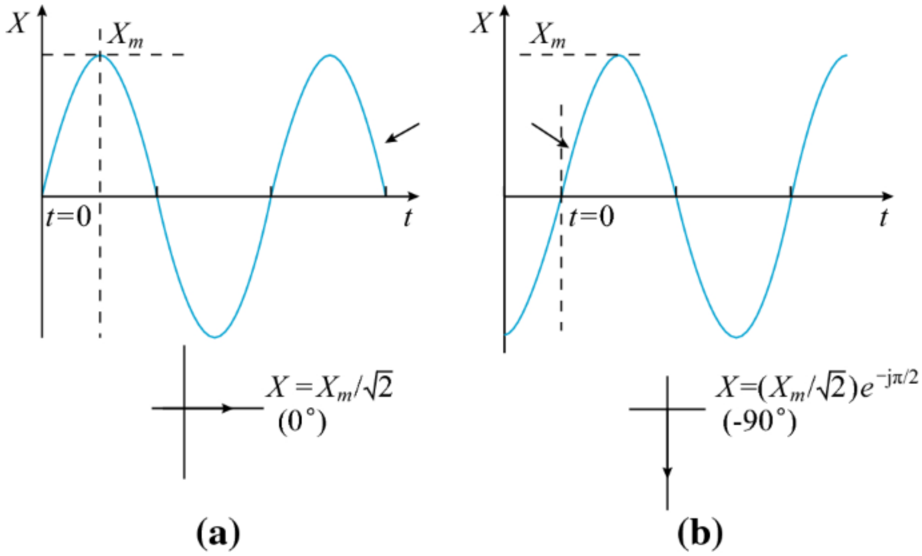

Figure 2.3: Convention for synchrophasor representation[39]

For a sinusoidal signal the phasor can be estimated by applying discrete Fourier transform (DFT) to the analog sampled system.

2.5.3 Discrete Fourier Transform

The discrete Fourier transform (DFT) is one of the most efficient techniques in digital computation. It is now at the heart of a lot of digital signal processing systems.

$$x(t) = X_m cos(2\pi f_0 t + \phi) \tag{2.3}$$

where X_m : maximum value of the input signal.

f_0: the nominal frequency.

ϕ_i : the initial phase angle of the input signal.

The signal has a Fourier series

$$\begin{aligned} x(t) &= a_k\, cos(2\pi f_o t) + b_k\, sin(2\pi f_o t) \\ &= \sqrt{a_k^2 + b_k^2}\ \ \cos(2\pi f_o t + \phi) \end{aligned} \tag{2.4}$$

where $\phi = arctan(\frac{b_k}{a_k})$

The signal is conventionally represented by a phasor related to the fundamental frequency component of its DFT is given by

$$X = \frac{X_m}{\sqrt{2}} \exp j\phi \tag{2.5}$$

where $X_m = \sqrt{a_k^2 +_b k^2}$

$$X = Xcos(\phi) + jXsin(\phi) \tag{2.6}$$

Assuming that the periodic signal x(t) is sampled N times (usually 12,24,36...) per fundamental period (50Hz or 60Hz with no harmonics n=1), the phasor representation (Fourier transform) is given by

$$X = \frac{\sqrt{2}}{N}(X_c - jX_s) \tag{2.7}$$

where $X_c = \sum_{K=1}^{N} X_k \cos\frac{2\pi}{N}K$ and $X_s = \sum_{K=1}^{N} X_k \sin\frac{2\pi}{N}K$

in some literatures, the definition of DFT with no harmonics is

$$X = \frac{\sqrt{2}}{N}\sum_{K=1}^{N} X_k \exp\frac{-j2\pi}{N}K \tag{2.8}$$

DFT can be divided into recursive and non-recursive methods of phasor estimation.

2.5.3.1 Non-recursive DFT

The non-recursive DFT is the simplest procedure to calculate phasors where the present output depends only on the present input its general equation is presented in 2.8.

For N number of samples per cycle the signal is sampled with sampling angle $\theta = \frac{2\pi}{N}$. This method requires 2N multiplications and 2(N-l) additions, therefore non-recursive algorithms are numerically stable but waste a lot of calculation time.

2.5.3.2 Recursive DFT

In this method the phasor is calculated for X^{N-1} and the next phasor (X^N) is calculated by updating the previous phasor recursively which reduce the number of multiplications because (N-1) multiplications by the Fourier coefficients are common to the new and old windows and this means that the sample (X_0) is removed and the sample (X_N) is added to the data set.

The general equation of recursive DFT is given by

$$\begin{aligned} X^N &= \frac{\sqrt{2}}{N}\sum_{K=0}^{N-1} X_{k+1} \exp\frac{-j2\pi}{N}(K+1) \\ &= X^{N-1} + \frac{\sqrt{2}}{N}(X_N - X_0)\exp\frac{-j2\pi}{N}0 \end{aligned} \tag{2.9}$$

where $\exp\frac{-j2\pi}{N}0 = \exp\frac{-j2\pi}{N}N$

$$X^{N+r} = X^{N+r-1} + \frac{\sqrt{2}}{N}(X_{N+r} - X_r)\exp\frac{-j2\pi}{N}r \tag{2.10}$$

Where r and (r-1) represent the present and the previous states respectively. If the measured signal is a constant sinusoidal.

In general, the recursive algorithm is faster, but it is numerically unstable. If a phasor estimating error occurs in one window, it will appear in all next phasors. For constant sinusoidal the phasor remains stationary in this estimation, in other words $X^{N+r} = X^{N+r-1}$ as long as $X_{N+r} = X_r$ [40].

2.6 Conclusion

From this chapter we can conclude that µPMU is a suitable device for measuring MGs voltage and current by dint of its architecture which offers a high speed and accurate synchrophasors in addition to the efficient mathematical tools (Non-recursive and recursive DFT) to extract these phasors. Therefore, the next chapter will introduce a proposed protection scheme using µPMU.

Chapter 3

Protection Scheme of MG

3.1 Introduction

The integration of MGs in power systems creates a new protection challenges, one of this challenges is the power direction .The power flow in the electric distribution system (EDS) is unidirectional in the absence of DGs. The addition of DGs to the EDS increases current short circuit and makes power flow bidirectional and increase the complexity of operating, controlling, and protecting medium (MV) and low voltage (LV) MGs [41]. Another challenge is the two modes of the MG."The conentional ovrecurrent protection system does not recognize the fault during islanded operation mode since it lies on the long-time tripping of overcurrent relay characteristics curve "[3].

This chapter presents an implemented MG protective system using PMU build of line parameters estimation method and smart protection algorithm.

3.2 Conventional Power System Protections

Protective relays and relaying systems automatically operate when they detect abnormal situations, such as failures in electrical circuits, to quickly isolate defective equipment from the system.

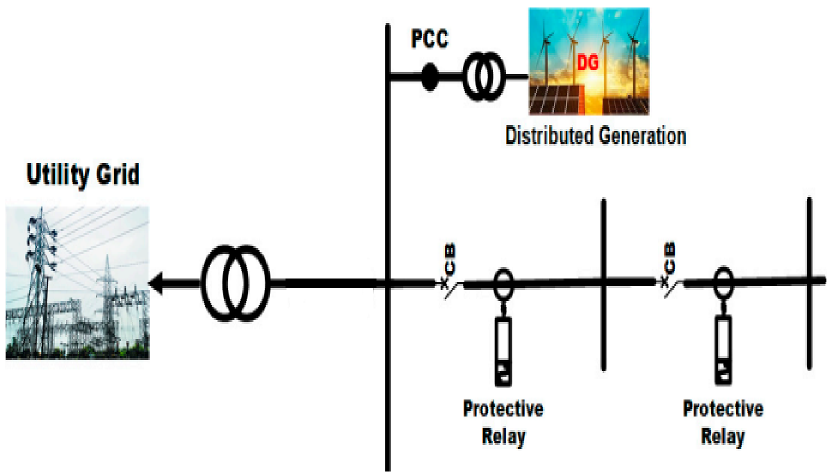

Figure 3.1: Conventional protections in power grid [27]

3.2.1 Differential Protection

One of the most used methods for power system protection is differential protection. It is based on the idea that the sum of all currents in the protected zone must always equal zero, with the exception of internal issues. Therefore, voltage measurements are not required which make this type of protection less sensitive to voltage variations and power swings[42].

3.2.2 Overcurrent Protection

Overcurrent protection relay has a set of predefined settings, their calculations take into account the maximum and minimum fault currents as well as the impedance of the feeders the relay is protecting in order to satisfy the protected network's criteria. These relays perform better for traditional distribution grids without DG. However, once DG is connected to the distribution network, protection relays may experience changes in the fault current level, and an incorrect trip decision may result [43].

3.3 Smart Protection System

Conventional protection systems are not sufficient to protect the new power systems (MG). Thus, adding a smart protection system (SPS) as a backup protection will increase the efficiency of the system protection.

In order to test the accuracy of the added SPS, a power system model has been used with multi-level fault scenario of short circuits and abnormalities.

3.3.1 Power System Model

Fig 3.2 presents the single line power system model, it is a LV and MV MG. The system contains integrated DGs (PV) in addition to MV synchronous motor as industrial loads and LV loads as residential loads.

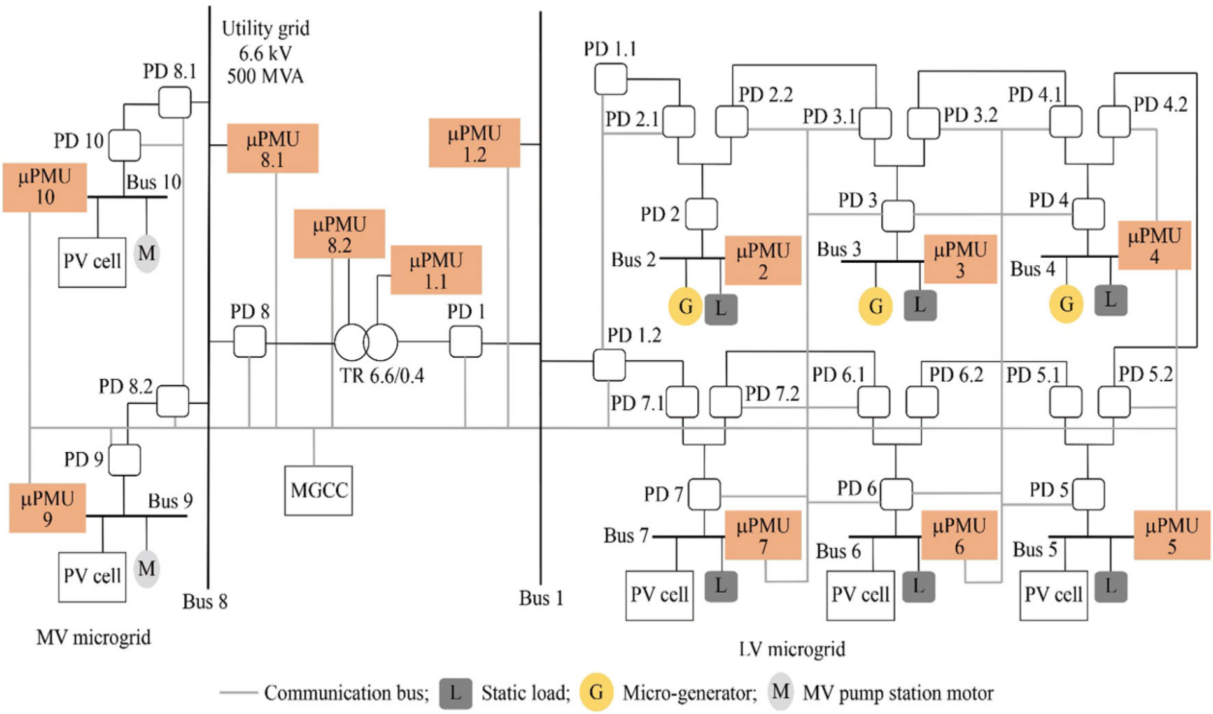

Figure 3.2: Single line diagram of MG model [3]

It is worth noting that due to the long time of simulation, the SPS will be tested in the LV part of the MG (bus 1 to bus 5).

3.3.2 µPMU Measurements

The following cases are different faults applying on different locations in the MG presented in Fig 3.2, the following conditions were taking into account:

- The two modes of the MG (grid-connected and islanded).
- The two states of micro-generator (On and Off).

The multi-events scenario used in testing the SPS were extracted from [3].

3.3.2.1 Case 1

This case represents the normal operation in grid-connected mode with PV cells fully loaded, and micro-generators OFF. The directional measurement data of this case are presented in Fig 3.3 and the PMU measurements in Table3.1.

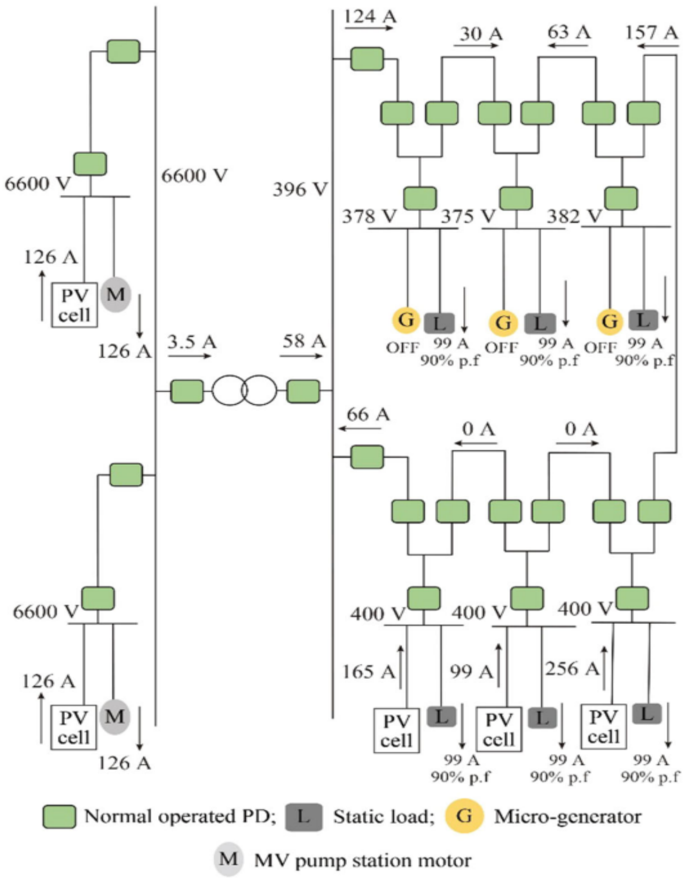

Figure 3.3: Directional measurement data of Case 1

Table 3.1: μPMU measurements of case 1

Bus	Voltage	Current
1	$V_1 = 396\underline{/-0.3}$	$I_{12} = 124\underline{/-27.2}$
2	$V_2 = 378\underline{/-0.8}$	$I_{21} = 124\underline{/-27.2}$ $I_{23} = 30\underline{/-27.2}$
3	$V_3 = 379\underline{/-0.9}$	$I_{32} = 30\underline{/-27.2}$ $I_{34} = 63\underline{/-26.6}$
4	$V_4 = 382\underline{/-0.6}$	$I_{43} = 63\underline{/-26.6}$ $I_{45} = 157\underline{/-26.4}$
5	$V_5 = 400\underline{/0}$	$I_{54} = 157\underline{/-26.2}$

3.3.2.2 Case 2

This case represents 3ϕ SC fault in grid-connected mode with PV cells fully loaded, and micro-generators ON (feeder 2-3). The directional measurement data of this case are presented in Fig 3.4 and the PMU measurements in Table3.2.

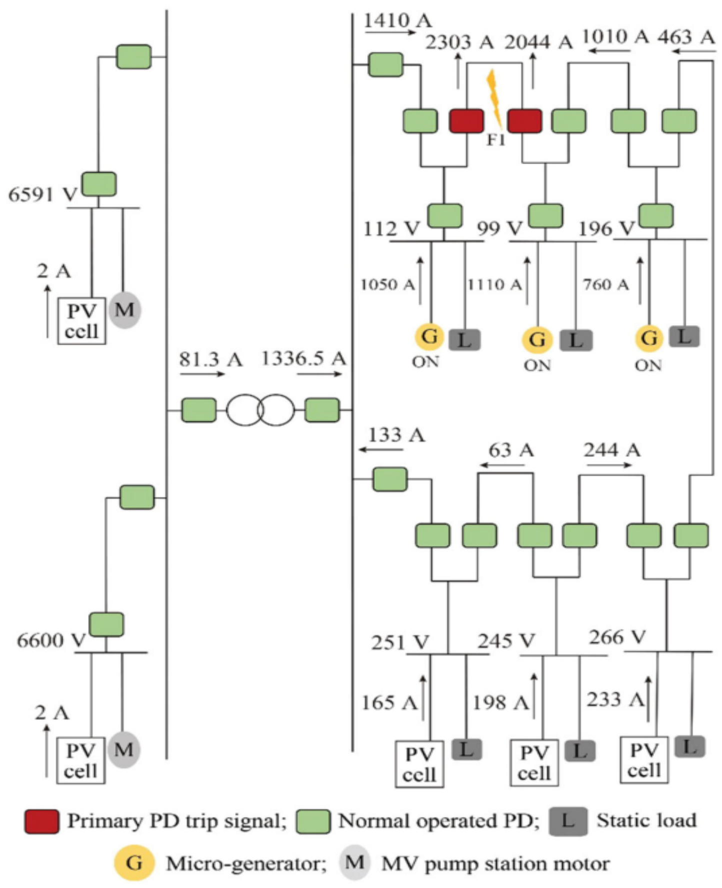

Figure 3.4: Directional measurement data of Case 2

Table 3.2: µPMU measurements of case 2

Bus	Voltage	Current
1	$V_1 = 246\underline{/-1.7}$	$I_{12} = 1412\underline{/-41.3}$
2	$V_2 = 112\underline{/-11.3}$	$I_{21} = 1412\underline{/-41.3}$ $I_{23} = 2030\underline{/-58.7}$
3	$V_3 = 100\underline{/-19.1}$	$I_{32} = 2040\underline{/-66.6}$ $I_{34} = 1010\underline{/-50.8}$
4	$V_4 = 196\underline{/-11.3}$	$I_{43} = 1010\underline{/-50.8}$ $I_{45} = 463\underline{/-5.58}$
5	$V_5 = 226\underline{/-2.1}$	$I_{54} = 463\underline{/-5.58}$

3.3.2.3 Case 3

This case represents 3ϕ SC fault in islanded mode with PV cells fully loaded, and micro-generators OFF (feeder 2-3). The directional measurement data of this case are presented in Fig 3.5 and the PMU measurements in Table3.3.

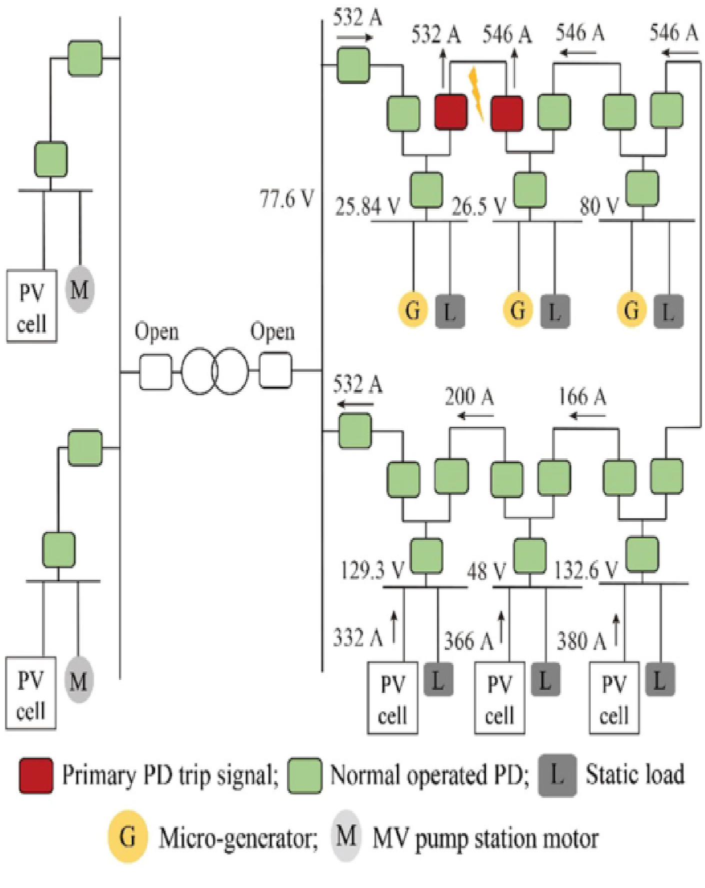

Figure 3.5: Directional measurement data of Case 3

Table 3.3: µPMU measurements of case 3

Bus	Voltage	Current
1	$V_1 = 77.6\underline{/32.8}$	$I_{12} = 532\underline{/-14.6}$
2	$V_2 = 25.84\underline{/3.8}$	$I_{21} = 532\underline{/-14.6}$ $I_{23} = 532\underline{/-14.6}$
3	$V_3 = 26.5\underline{/32.8}$	$I_{32} = 546\underline{/-14.6}$ $I_{34} = 546\underline{/-14.6}$
4	$V_4 = 80\underline{/32.8}$	$I_{43} = 546\underline{/-14.6}$ $I_{45} = 546\underline{/-14.6}$
5	$V_5 = 132.64\underline{/32.8}$	$I_{54} = 546\underline{/-14.6}$

3.3.2.4 Case 4

This case represents 3ϕ SC fault on islanded mode with PV cells OFF, and micro-generators ON (feeder 3-4). The directional measurement data of this case are presented in Fig 3.6 and the PMU measurements in Table3.4.

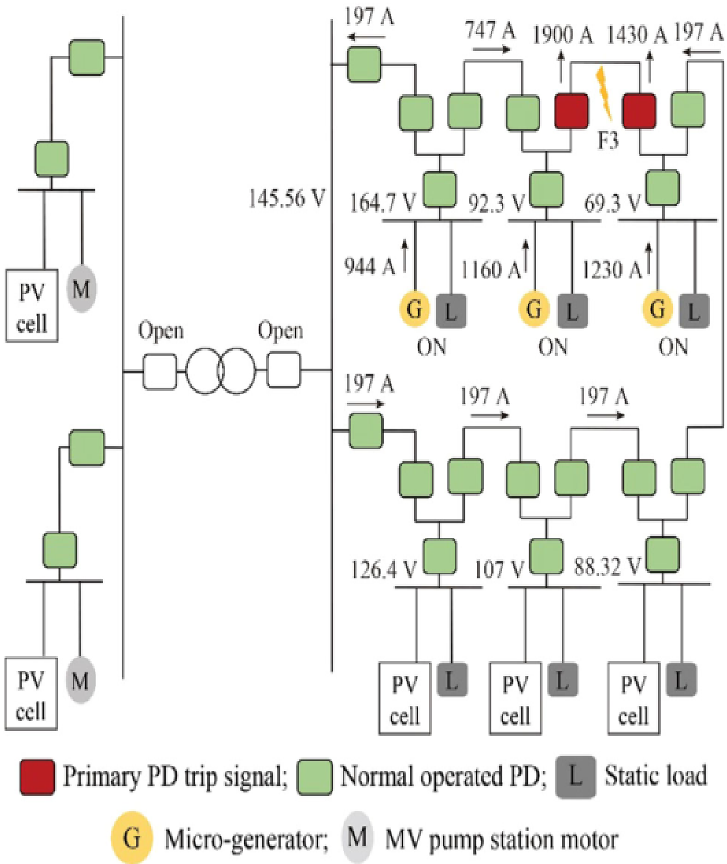

Figure 3.6: Directional measurement data of Case 4

Table 3.4: µPMU measurements of case 4

Bus	Voltage	Current
1	$V_1 = 145.6\underline{/-26.9}$	$I_{12} = 197\underline{/-69.8}$
2	$V_2 = 164.7\underline{/-26.4}$	$I_{21} = 197\underline{/-69.8}$ $I_{23} = 747\underline{/-71.1}$
3	$V_3 = 92.3\underline{/-28.5}$	$I_{32} = 747\underline{/-71.1}$ $I_{34} = 1900\underline{/-76}$
4	$V_4 = 69.3\underline{/31.9}$	$I_{43} = 1430\underline{/-79.3}$ $I_{45} = 197\underline{/-69.8}$
5	$V_5 = 88.3\underline{/-29.9}$	$I_{54} = 197\underline{/-69.8}$

3.3.3 Line Parameters Estimation

The line impedance and admittance parameters are calculated using current and voltage measurements provided by PMU at the end of each bus [44].

$$\begin{aligned}[V_m] &= [T_I]^t[V] \\ [I_m] &= [T_I]^{-1}[I]\end{aligned} \tag{3.1}$$

where V_m and I_m are the measured current and voltage in modal domain and m is the number of phases [45].

$$[T_I] = \begin{bmatrix} 1 & 1 & 1 & \dots & 1 \\ 1 & 1-m & 1 & \dots & 1 \\ 1 & 1 & 1-m & \dots & 1 \\ . & . & . & & . \\ . & . & . & & . \\ . & . & . & & . \\ 1 & 1 & 1 & \dots & 1-m \end{bmatrix} \tag{3.2}$$

$$[T_I]^{-1} = \frac{1}{m} \begin{bmatrix} 1 & 1 & 1 & \dots & 1 \\ 1 & -1 & 0 & \dots & 0 \\ 1 & 0 & -1 & \dots & 1 \\ . & . & . & & . \\ . & . & . & & . \\ . & . & . & & . \\ 1 & 0 & 0 & \dots & -1 \end{bmatrix} \tag{3.3}$$

The relation between complex currents and voltages is given by:

$$V_A = V_B \cosh \gamma_k d - I_B Z_{ck} \sinh \gamma_k d \tag{3.4}$$

$$I_A = -I_B \cosh \gamma_k d + \frac{V_B}{Z_{ck}} \sinh \gamma_k d \tag{3.5}$$

where γ_k and Z_{ck} are, respectively, the propagation function and characteristic impedance of the k-th mode, and d is the length of the bus in Km.

$$\gamma_K = \frac{1}{d} \frac{V_A I_A - V_B I_B}{V_B I_A - V_A I_B} \tag{3.6}$$

$$Z_{ck} = \frac{V_B \sinh \gamma_K}{I_A + I_B \cosh \gamma_K} \tag{3.7}$$

The longitudinal impedance and transversal admittance of the k-th mode can be calculated as follow :

$$\begin{aligned} Z_m &= \gamma_K Z_C \\ Y_m &= \frac{\gamma_K}{Z_C} \end{aligned} \tag{3.8}$$

$$\begin{aligned} [Z_m] &= \begin{bmatrix} Z_{m1} & 0 & 0 \\ 0 & Z_{m2} & 0 \\ 0 & 0 & Z_{m3} \end{bmatrix} \\ [Y_m] &= \begin{bmatrix} Y_{m1} & 0 & 0 \\ 0 & Y_{m2} & 0 \\ 0 & 0 & Y_{m3} \end{bmatrix} \end{aligned} \tag{3.9}$$

The last step is a transformation from modal domain to phase domain of the longitudinal impedance and transversal admittance matrices, it is defined as follow:

$$\begin{aligned} [Z] &= [T_I]^{-t} [Z_m] [T_I]^{-1} \\ [Y] &= [T_I] [Y_m] [T_I]^t \end{aligned} \tag{3.10}$$

3.3.4 Protection Algorithm

This protection is based on the synchronized PMU measurements of the 3ϕ current and voltage at the sending (A) and receiving(B) end buses.

As first step of calculation, each 3ϕ synchronized signal (V_a, V_b, V_c) is transferred to a decoupled phase components

(V_α, V_β, V_0) using clarke transformation, this transformation is presented mathematically as:

$$\begin{bmatrix} V_a \\ V_b \\ V_c \end{bmatrix} = T_{Clarke} \begin{bmatrix} V_\alpha \\ V_\beta \\ V_0 \end{bmatrix}$$
$$\begin{bmatrix} I_a \\ I_b \\ I_c \end{bmatrix} = T_{Clarke} \begin{bmatrix} I_\alpha \\ I_\beta \\ I_0 \end{bmatrix} \tag{3.11}$$

where

$$T_{Clarke} = \begin{bmatrix} \frac{2}{\sqrt{6}} & 0 & \frac{1}{\sqrt{3}} \\ -\frac{1}{\sqrt{6}} & \frac{1}{\sqrt{2}} & \frac{1}{\sqrt{3}} \\ -\frac{1}{\sqrt{6}} & -\frac{1}{\sqrt{2}} & \frac{1}{\sqrt{3}} \end{bmatrix} \tag{3.12}$$

Therefore, the D_{index} and the abnormality coefficient are calculated for detecting SCs, overvoltage, undervoltage and overload. If a fault occurs, the MG central controller (MGCC) will send a trip signals to the protection devices (PDs).

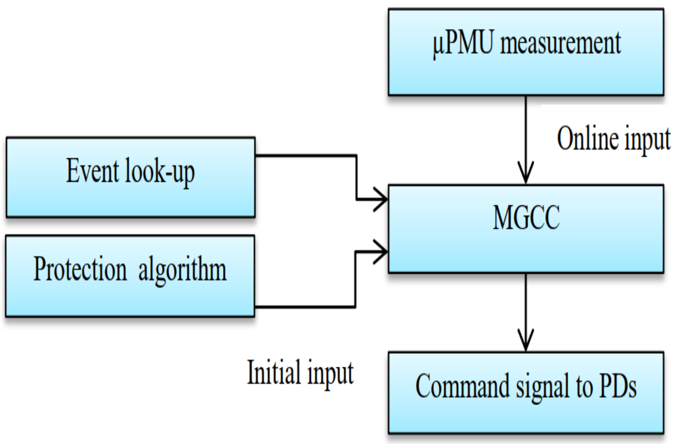

Figure 3.7: Operational function of MGCC

The statue of the D_{index} depends of the situation of each feeder. If the magnitude of any component of the D_{index} converges to exist instantly, the feeder is considered defective and if it tends to infinity or it does not exist, the feeder is healthy. The abnormality coefficient γ of each bus is calculated in the MGCC. If the overloading factor O_i is equal to or greater than 1 or if the bus overvoltage coefficient O_V is greater than 1.15, or if the bus undervoltage coefficient U_V is less than 0.85, the MGCC sets a logic value of "1" to the γ coefficient.

$$D_{ij} = D_\alpha + D_\beta + D_0$$
$$\gamma_i = O_i + O_V + U_V \tag{3.13}$$

Table 3.5: Event look-up table

D_{ij}	γ_i	Event
0	0	Normal Operation
0	1	Abnormal Case
1	0	SC Fault Case
1	1	Fault and Abnormal Case

3.3.4.1 Fault Index

The SC factor or the D_{index} is calculated through many steps. The equations that describes these steps are presented mathematically as follow :

$$D(i) = \frac{\ln \frac{A(i)-C(i)}{E(i)-B(i)}}{2\Gamma(i,i)L} \tag{3.14}$$

$$Z_C(i) = \frac{V_{Am}^2 - V_{Bm}^2}{I_{Am}^2 - I_{Bm}^2} \tag{3.15}$$

The propagation index Γ is expressed in equation 3.16 as:

$$\Gamma = \sqrt{T^{-1}ZYT} \tag{3.16}$$

Where Z and Y are line impedance and admittance matrices respectively. A(i), B(i), C(i), and E(i) are entries vectors defined by:

$$A(i) = \frac{V_{Bm}(i) + Z_C(i)I_{Bm}(i)}{2} \tag{3.17}$$

$$B(i) = \frac{V_{Bm}(i) - Z_C(i)I_{Bm}(i)}{2} \tag{3.18}$$

$$C(i) = \frac{V_{Am}(i) + Z_C(i)I_{Am}(i)}{2\exp\Gamma(i,i)L} \tag{3.19}$$

$$E(i) = \frac{V_{Am}(i) - Z_C(i)I_{Am}(i)}{2\exp\Gamma(i,i)L} \tag{3.20}$$

Fig 3.8 is the flowchart of the protection system, where the µPMU A and B are the µPMUs at the end of the sending and receiving buses respectively. For each sample all the calculation steps presented in this chapter will be provided as ordered in the flowchart.

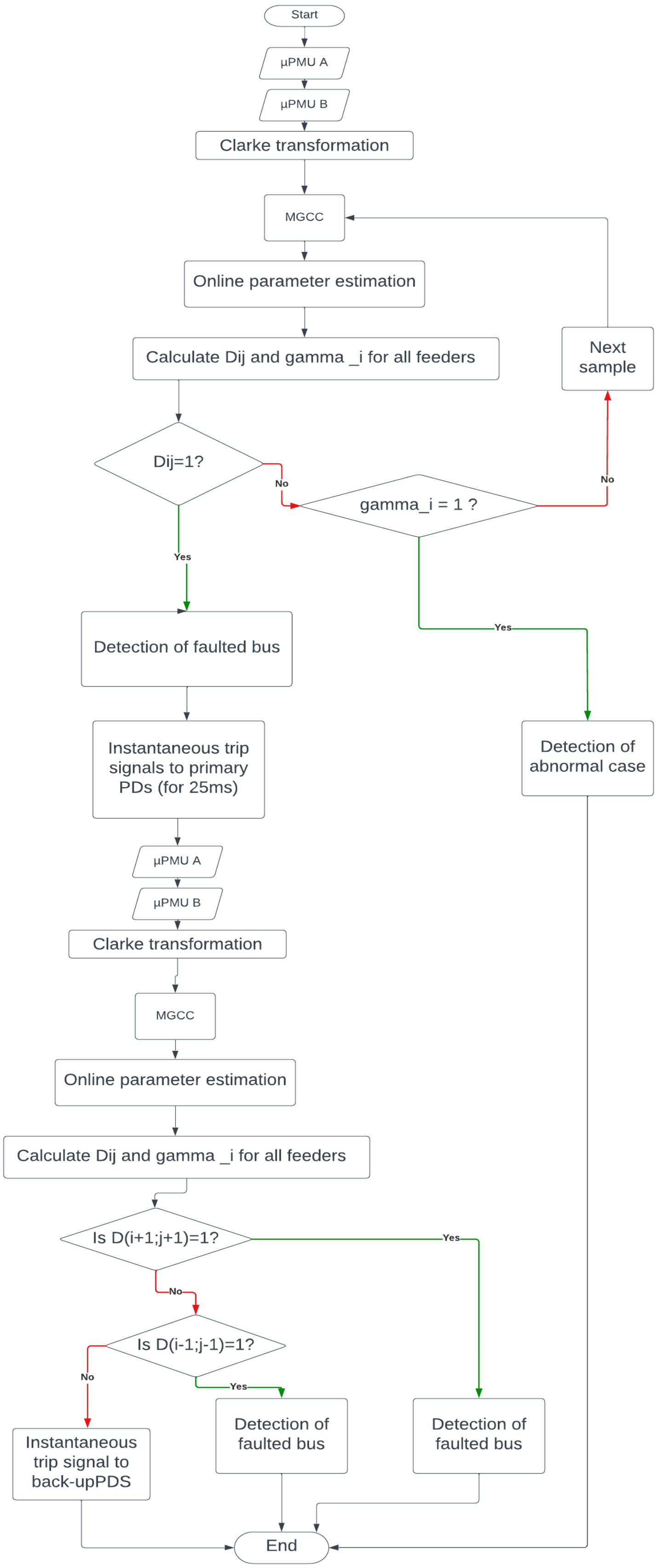

Figure 3.8: Flowchart of proposed protection algorithm

3.3.4.2 Protection results

The MGCC will make the decision of the PD (circuit breaker) state and send the trip signal to the PDs according to Table 3.6.

Table 3.6: Protection algorithm results

Case	D_{ij}	γ_i	Event Detection	PD status
1	$D_{ij} = 0$	$\gamma_i = 0$	Normal Operation	All PDs are closed
2	$D_{23} = 1, D_{ij} = 0$	$\gamma_i = 1$	3-$\phi faultonfeeder2-3$	trip signal to PB 2.2 and PD 3.1
3	$D_{23} = 1, D_{ij} = 0$	$\gamma_i = 1$	3-$\phi faultonfeeder2-3$	trip signal to PB 2.2 and PD 3.1
4	$D_{34} = 1, D_{ij} = 0$	$\gamma_i = 1$	3-$\phi faultonfeeder3-4$	trip signal to PB 3.2 and PD 4.1

3.3.4.3 Simulation Software Choice

The smart protection system (SPS) is based on multi-level continuous matrices operations and equations calculations. Thus, the simulation software must involve the following characteristics:

- System-level design.
- Continuous test and verification.
- Matrices and equation calculations.
- High accuracy signal display.

Therefore, the Simulink software is used to simulate the SPS protection algorithm block model (mdl) . This program model is designed using existing Simulink libraries, a modified PMU Simulink developed sub-system [40], and the SPS sub-system block.

3.4 Conclusion

This chapter presents the theoretical part of the protection. It has been tested in a LV MG under different fault scenarios for the grid-connected and the islended mode.

Model domain and clarke transformations have been used in order to calculate the different parameters (voltages, currents and line characteristics).

Chapter 4

Simulation and Results

4.1 Introduction

This chapter covers basically the SPS block diagram design along with the sub-system blocks of the mathematical models of the line characteristics estimation and the SPS, also it presents the simulation results and their discussion.

4.2 Smart Protection System Block Diagram

The protection modal is composed of two main blocks, the first one is for generating the testing scenario and the second one is the design of smart protection system model.

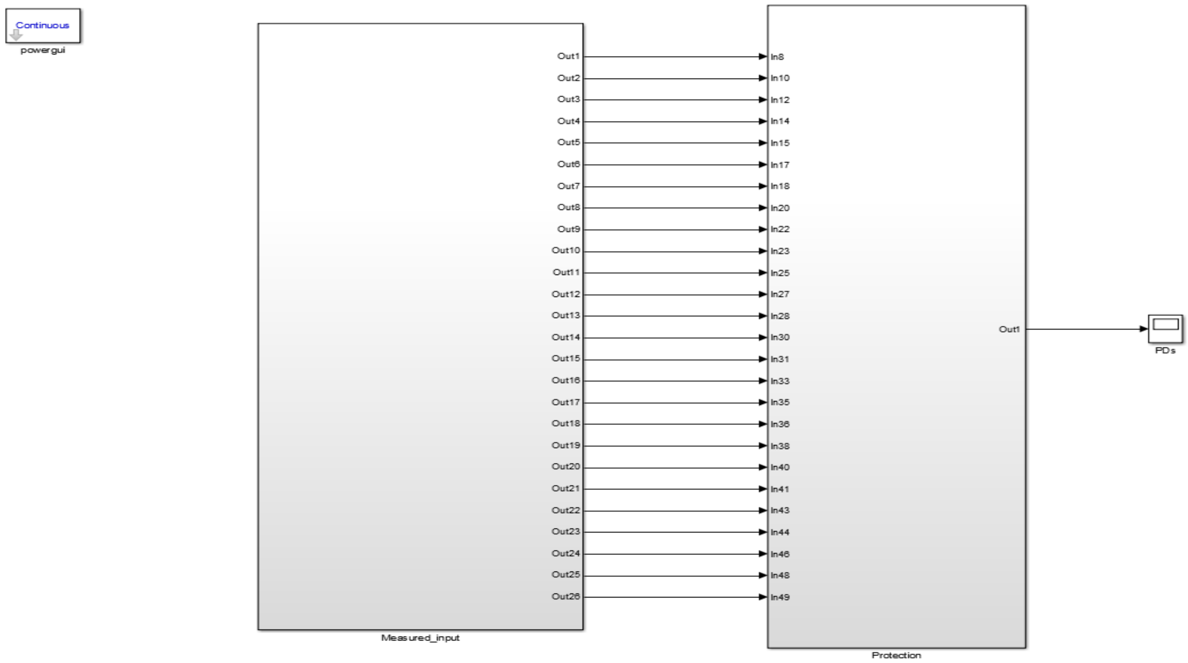

Figure 4.1: Smart Protection System Block Diagram

4.2.1 Generated Signals Block Diagram

The first block diagram is designed in order to generate the 3ϕ signals. As Fig 4.2 shows, the current and voltage signals are generated separately. Table 4.1 summaries the events time period used for testing this SPS, it is generated based on different faults combined in one multi-event scenario.

Table 4.1: Generated scenario

Case number	Time period (second)
1	0-10 12-17 19-29 31-36
2	10-12
3	17-19
4	29-31

The three phase voltage/current generator has been used for signal generation. This signal will pass through the µPMU subsystem where their phasors will be calculated. After that, the extracted phasors will be converted from the abc form to alpha- beta-zero form using abc to alpha-beta-zero block. Fig 4.2 shows the designed model for generating V_4, I_{43} and I_{45}.The currents and voltages values of each case of the scenario have been presented in the chapter 3.

4.2.1.1 µPMU Working Principle

As explained in chapter 2, the µPMU is designed based on DFT. In [46] a DFT simulink model was developed.

After the discretization of the generated analog signal and using the Fourier coefficients calculated priorly based on the used sampling frequency, the DFT algorithm performs a loop calculation for one cycle (fundamental frequency) to estimate the phasors which are the RMS magnitude and phase angle of the measured analog signal.

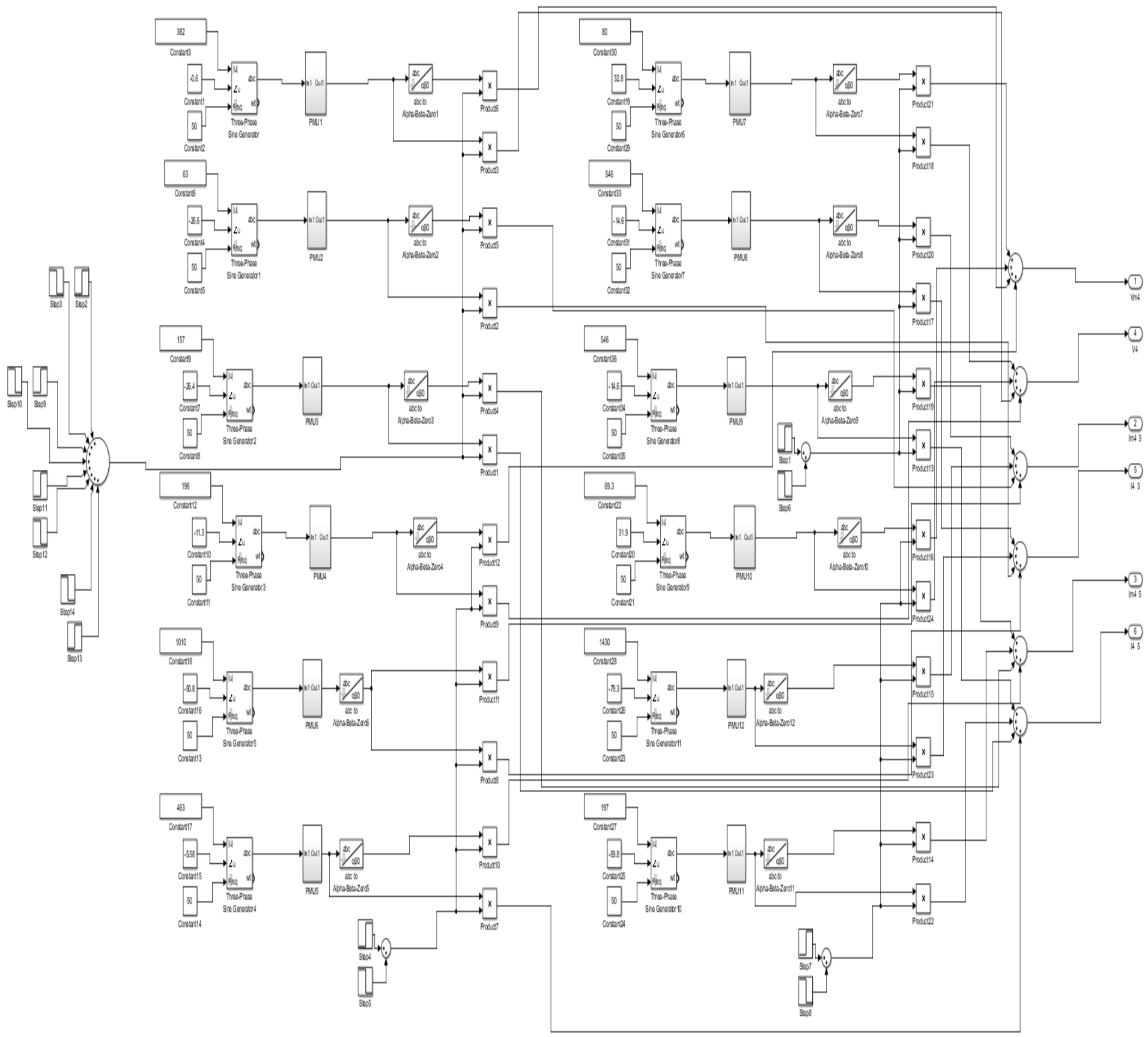

Figure 4.2: V_4, I_{43} and I_{45} signals model

4.2.2 SPS Block Diagram

The second block diagram represents the SPS algorithm. It consists of building sub-blocks, where each one represents a step calculation mathematically modeled by the set of equations (3.14 to 3.20) developed in chapter 3. The sub-blocks are connected to follow step calculation in correct order as described in the algorithm flowchart.

To summarize, the inputs to SPS protection block are the inputs voltage/current obtained from the PMU place in important network nodes and the outputs are PDs status of the complete MG network.

Both 3ϕ signals and clarke components are needed in this part. The 3ϕ signals are used in calculating lines characteristics and feeders γ coefficient, however, the clarke components are used in calculating the feeders D_{index}.

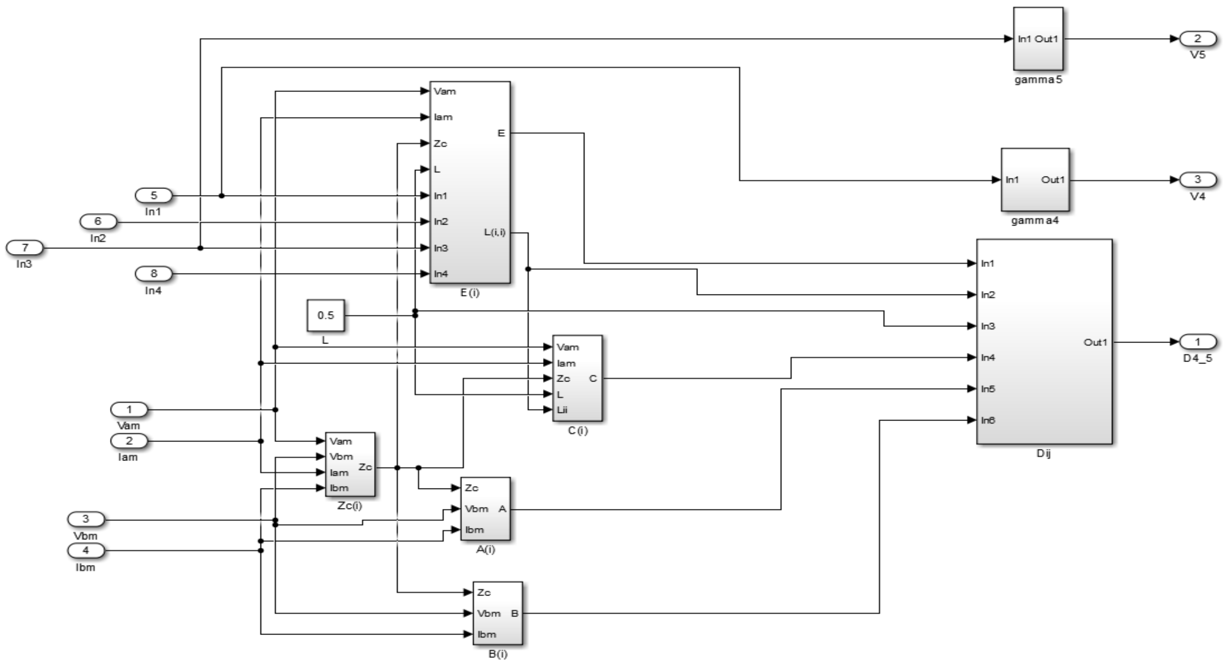

Figure 4.3: Protection diagram

4.2.2.1 The γ Coefficient

After calculating the numeric values the γ coefficient of each feeder, its boolean state will be derived using compare to constant blocks. Fig 4.4 is the inner design of γ_3 subsystem shown in Fig 4.3, where the values of the constants represent the base voltage and current in the LV MG.

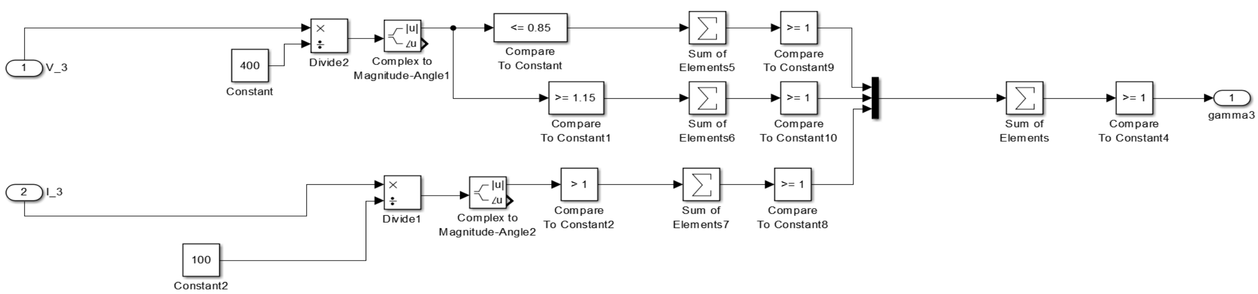

Figure 4.4: γ_3 block diagram

4.2.2.2 PDs State Estimation

The final stage of the protection is about estimating the PDs status according to the calculated feeders D_{index}. This estimation is summarized in Table 3.6.

The PDs state is obtained using switches as Fig 4.5 shows. From flowchart illustrated in Fig 3.8, a trip signal will be sent to the PDs of the faulted feeder and the feeders connected to it, after a delay of 25ms a back-up trip signal will be sent to the PDs of the non-faulted feeders, this method allows the MGCC to detect the location of the fault and isolate the bus.

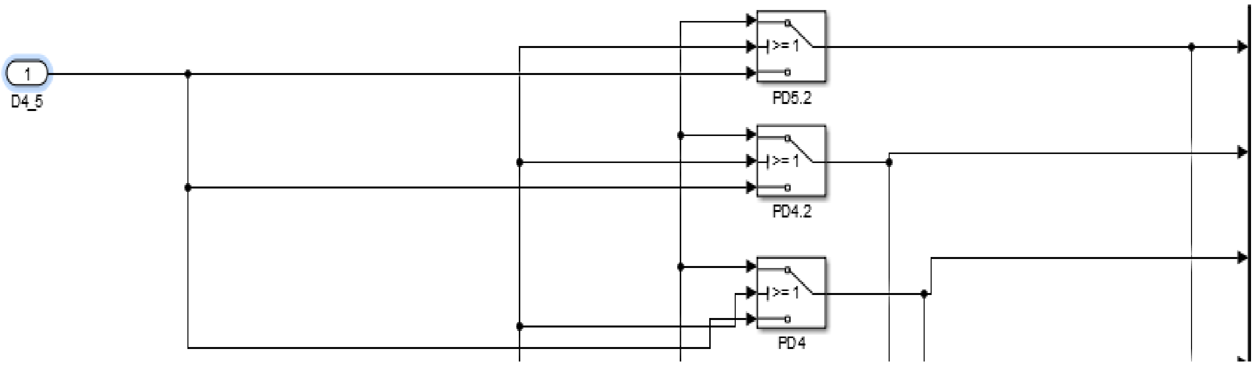

Figure 4.5: PD_{52}, PD_{42} and PD_4 state estimation

4.3 Simulation Results

4.4 The Generated Signals

The generated 3ϕ sinusoidal input signal of bus 2 is presented in Fig 4.6, it illustrates the fault occurs in case 2.

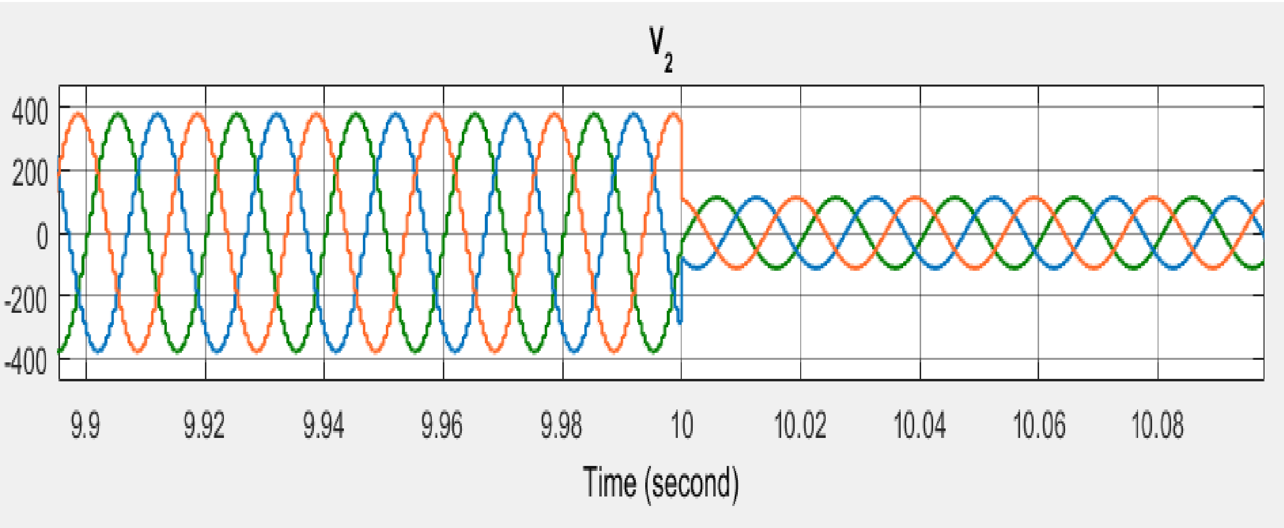

Figure 4.6: Input Signal V_2

4.4.1 µPMU Measurements

Fig 4.7 presents the voltage phasors measurements of each bus provided by the µPMU model in terms of magnitude and phase. Fig 4.8 illustrates the fault occurring in bus 2 at t=10s, and this proves the accuracy of the µMPU and makes it a suitable device to be used in protection systems.

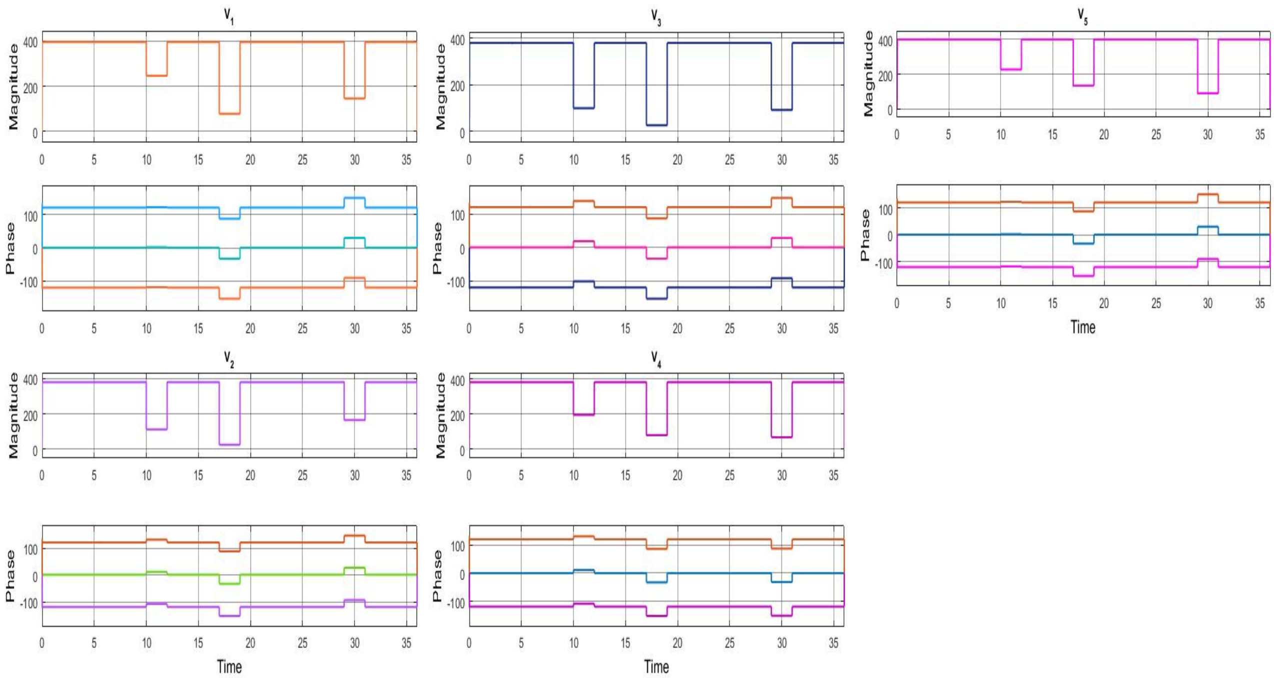

Figure 4.7: μPMU voltage measurements

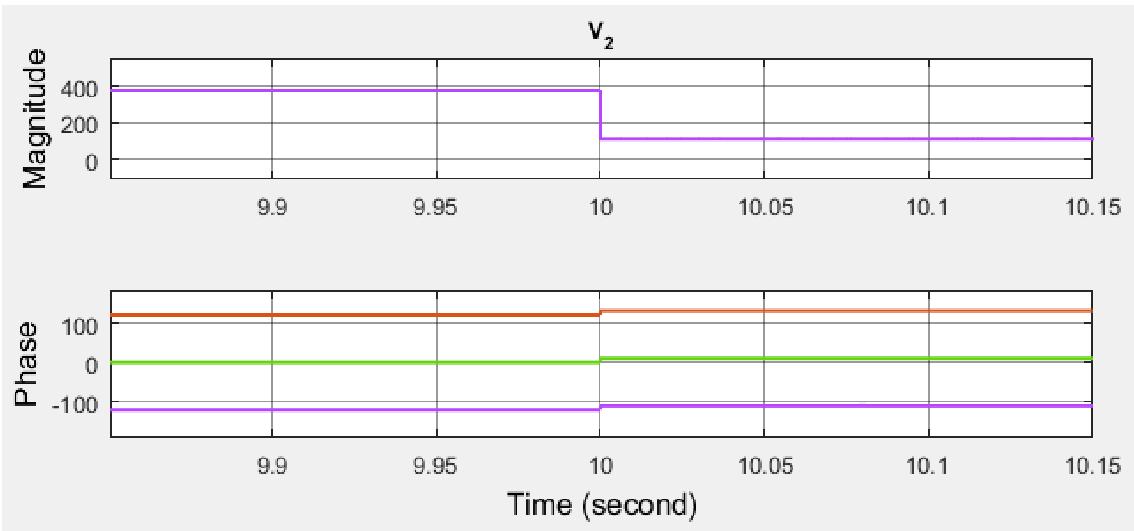

Figure 4.8: μPMU measurements of V_2 in case 2

4.4.2 Clarke Components

As can be seen in Fig 4.9 the results of clarke transformation has only two components which will simplify the calculations of the protection parameters, clear demonstration of the obtained results is presented in Fig 4.10 and **??**
.

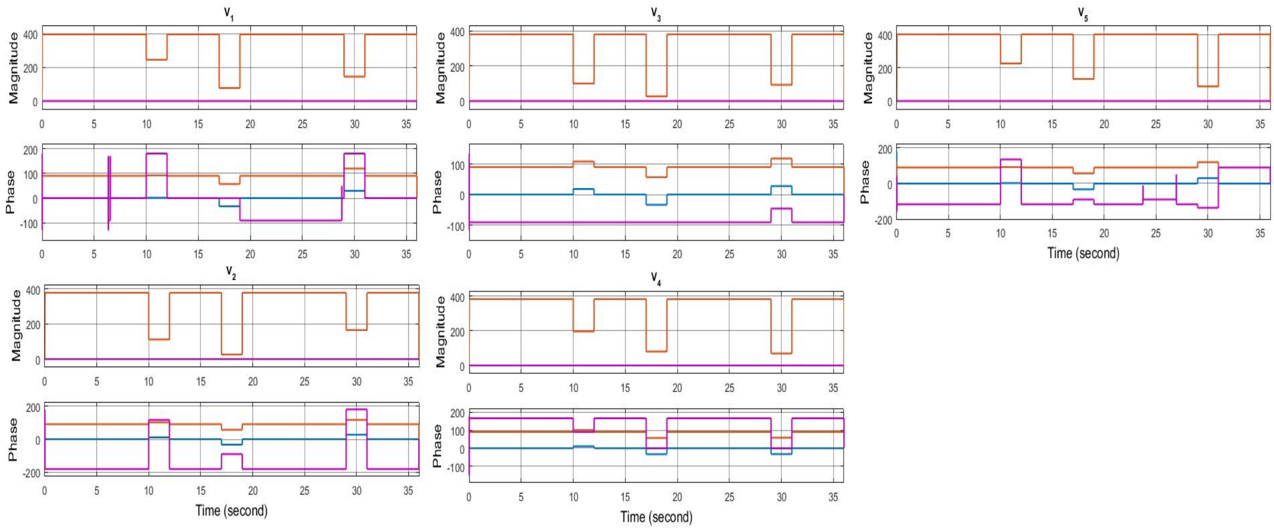

Figure 4.9: Voltage Clarke components

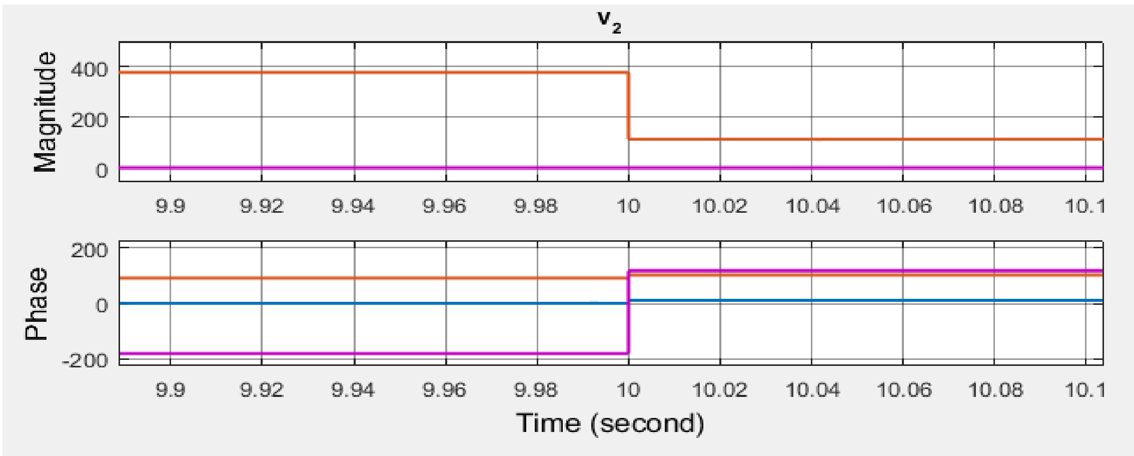

Figure 4.10: Clarke components of V_2 in case 2

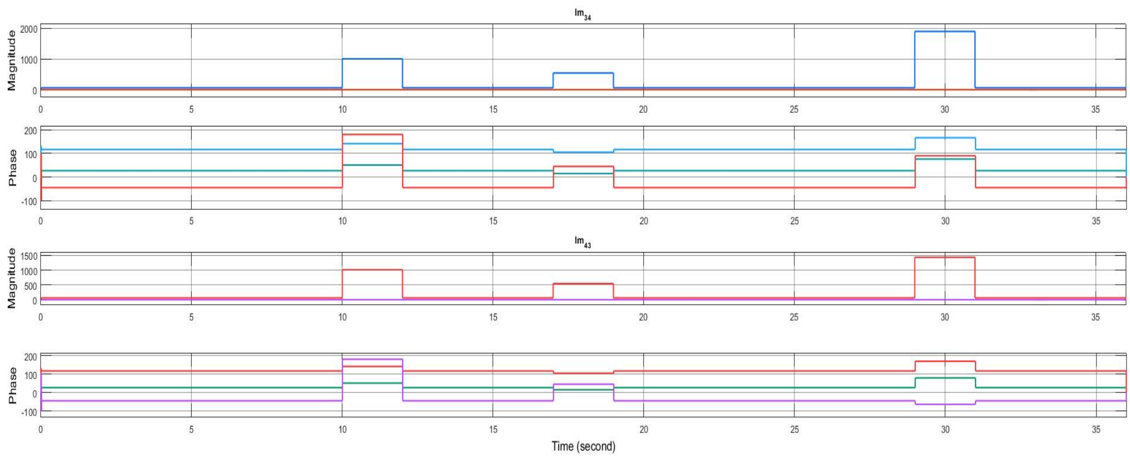

Figure 4.11: Clarke components of I_{23} and I_{23} in case 2

4.5 PDs State

As explained in the chapter 3, the PDs state depends on the boolean state of the feeders D_{index}. Fig 4.12 presents the numeric values of D_{12}. The PDs of the network are presented in Fig 4.14.

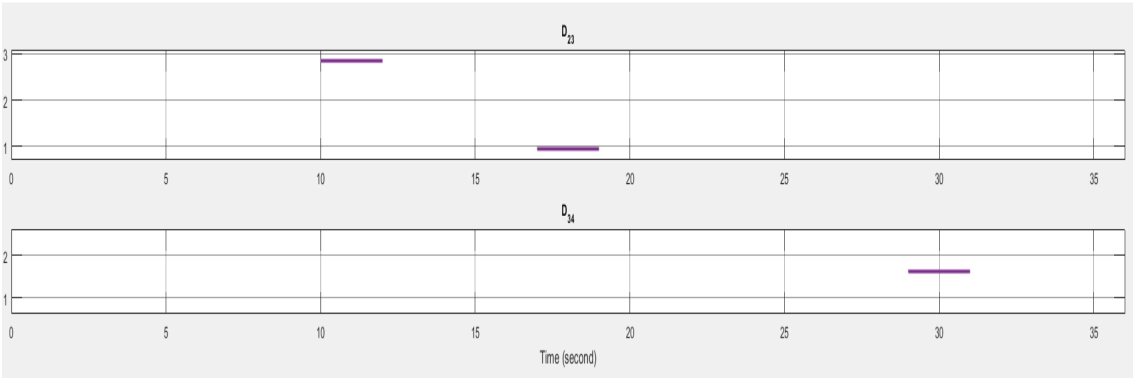

Figure 4.12: D_{12} numeric values

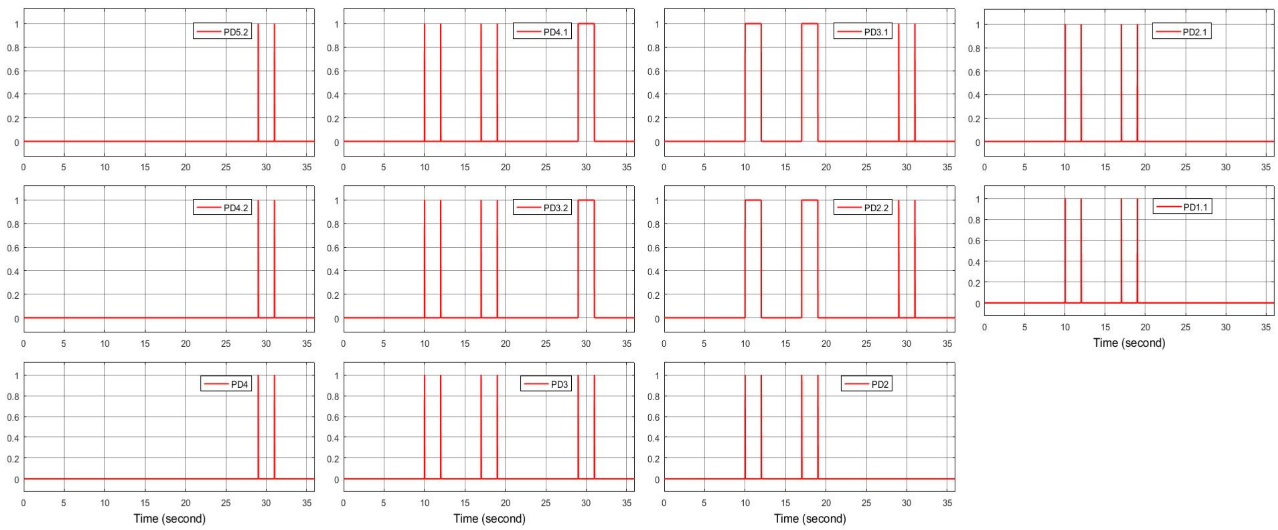

Figure 4.13: PDs

Fig 4.14, 4.15 and 4.17 present the PDs state for each case. As can be seen,the obtained results are compatible with the protection results presented in table 3.6. This results show the fast response of the protection to sc faults, which is very important for such type of protections in order to isolate the faulted bus and protect the maximum area of the MG.

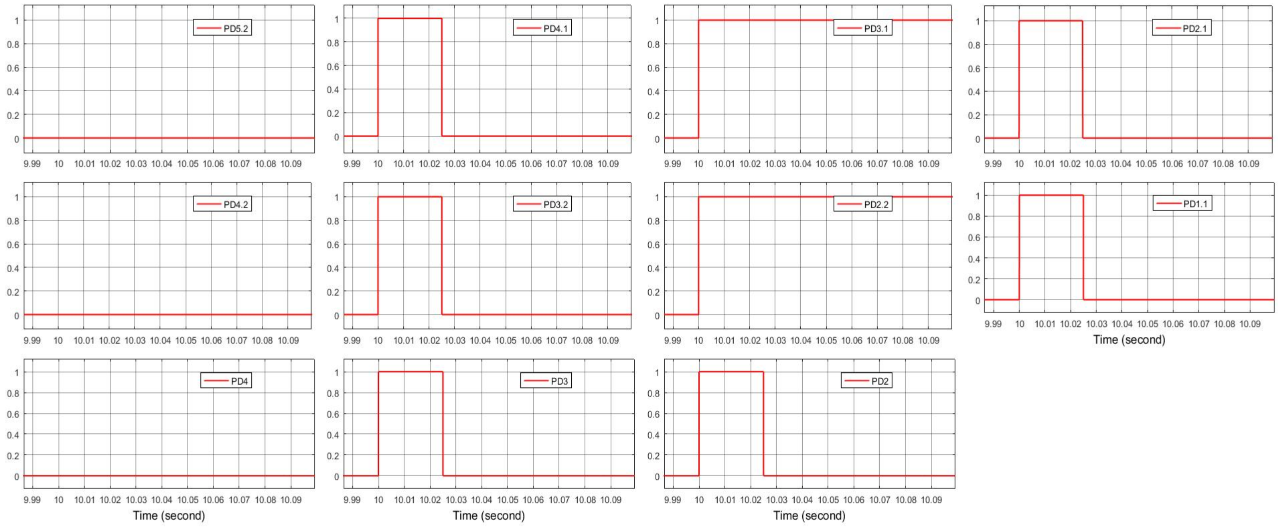

Figure 4.14: PDs case 2

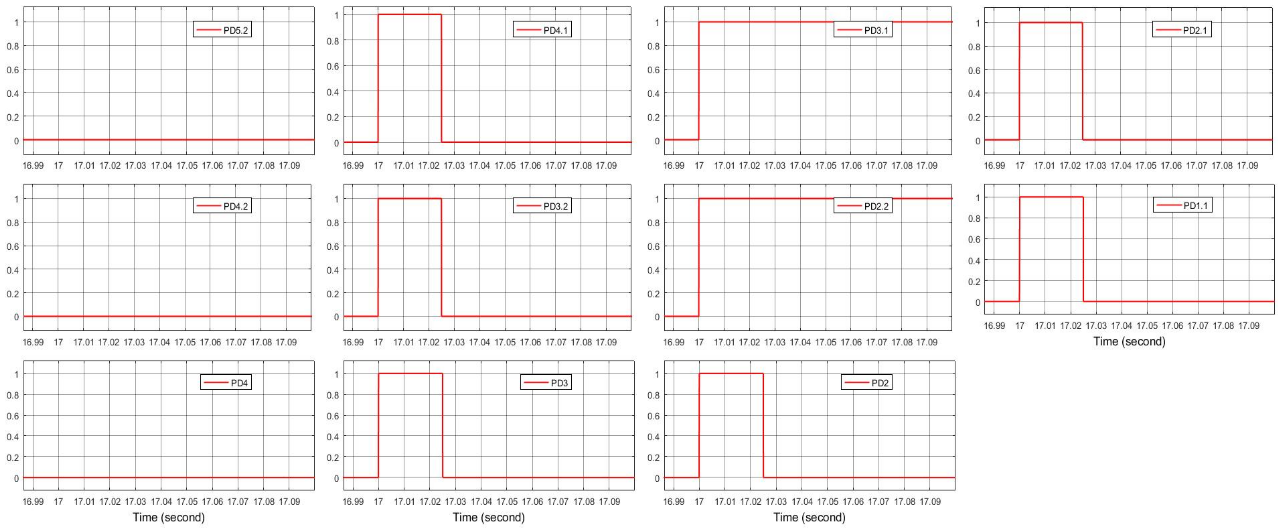

Figure 4.15: PDs case 3

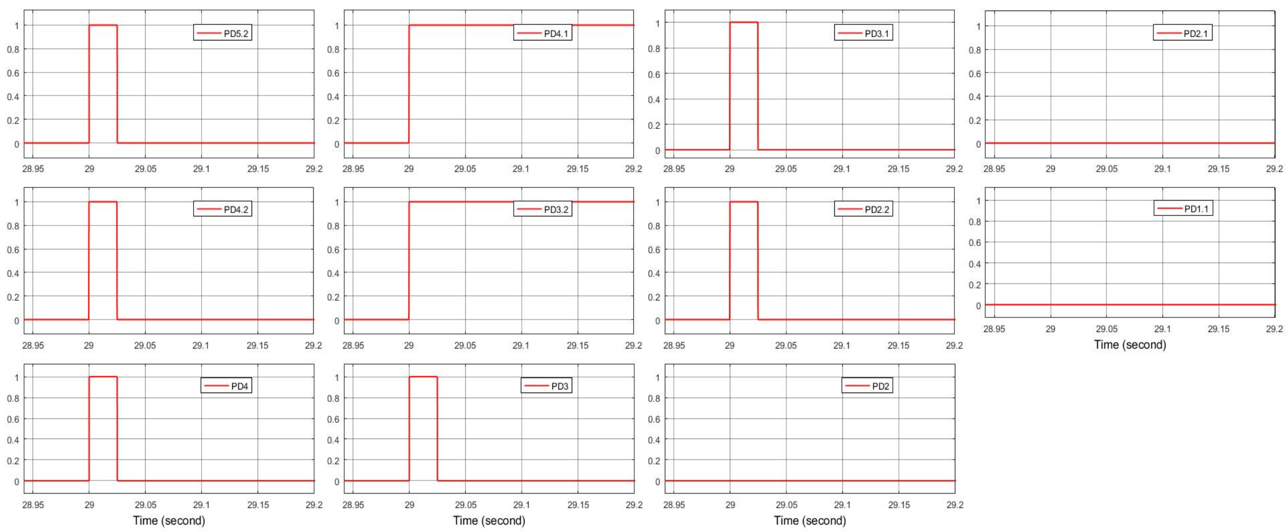

Figure 4.16: PDs case 4

4.5.1 The abnormality coefficient γ

The detection of abnormality events such as overcurrent, undervoltage and overvoltage is very important to supervise power systems. Fig 4.17 exposes the results of the γ_3 provided by this SPS.

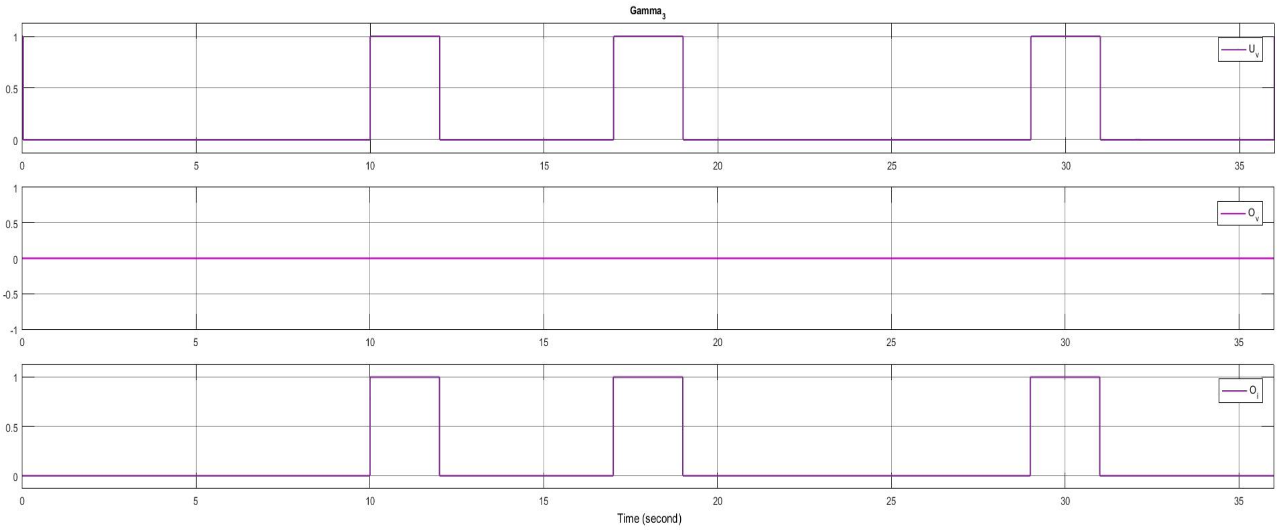

Figure 4.17: γ_3 coefficient

4.6 Conclusion

The protection was tested successfully in the proposed scenario and provided accurate results.

The PDs were responding correctly to the faulted situations without disturbing the performance of the network. This protection was able to isolate the faulted bus and protect the buses connected to it.

General Conclusion

MGs are becoming more and more prevalent because of their ability to use renewable energy sources and keep electricity supplied without destroying nature. This integration may cause new issues at the protection level of power systems which require new solutions. One of this solutions is the SPS.

The SPS function uses the voltages/currents input data received from µPMUs at each node of the MG. After that, the algorithm of the SPS derives the PD states at each node of the distributed power grid (MG) by following ordered step calculations . The derived output in fact constitutes the new states (ON or OFF) of the PDs status, The obtained results are sent to the distributed PDs at the different locations of the MG based on standardized communication protocols as IEC6 1850. This SPS has been tested using a multi-event scenario, to test the different abnormal conditions and SC faults at different positions of the distribution power grid. Good results have been obtained, the state of the PD at the faulted section is generated as expected, also a clear supervision of the power system has been provided.

As further work to this project, the SPS seems to be able to detect other types of SCs such as line to line and line to ground faults. On the other hand, the numerical values of the D_{index} may have valuable meaning and it may be used to detect the type of the SC fault .

References

[1] A. Aktas and Y. Kircicek, *Solar Hybrid Systems: Design and Application*. Elsevier Science, 2021, ISBN: 9780323884990. [Online]. Available: `https://books.google.dz/books?id=gNIqEAAAQBAJ`.

[2] H. Nikkhajoei and R. H. Lasseter, "Microgrid protection," in *2007 IEEE Power Engineering Society General Meeting*, IEEE, 2007, pp. 1–6.

[3] M. S. Elbana, N. Abbasy, A. Meghed, and N. Shaker, "μPmu-based smart adaptive protection scheme for microgrids," *Journal of Modern Power Systems and Clean Energy*, vol. 7, no. 4, pp. 887–898, 2019.

[4] *Bridgestone associates*, https://brdgstn.com/microgrid, June, 2022.

[5] S. Kottayil, *Smart Micro Grid*, ser. Smart Microgrids. CRC Press, 2020, ISBN: 9780367343620. [Online]. Available: `https://books.google.dz/books?id=jJFuzQEACAAJ`.

[6] K. Cabana-Jiménez, J. E. Candelo-Becerra, and V. Sousa Santos, "Comprehensive analysis of microgrids configurations and topologies," *Sustainability*, vol. 14, no. 3, p. 1056, 2022.

[7] T. T. SON, "Islanding detection and power quality analysis in microgrid," Ph.D. dissertation, SHIBAURA INSTITUTE OF TECHNOLOGY, 2019.

[8] M. M. I. Abd El-Rahman, "Optimization of renewable energy-based smart micro-grid system," *Modeling, Simulation and Optimization of Wind Farms and Hybrid Systems*, p. 225, 2020.

[9] S. Das, M. Islam, and W. Xu, *Advances in Control Techniques for Smart Grid Applications*. Springer Nature Singapore, 2022, ISBN: 9789811698569. [Online]. Available: `https://books.google.dz/books?id=P99mEAAAQBAJ`.

[10] *Our world in data, renewable energy*, https://ourworldindata.org/renewable-energy, 2022.

[11] C. Xie, J. Wang, B. Luo, X. Li, and L. Ja, "A control strategy for battery/supercapacitor hybrid energy storage system," in *Journal of Physics: Conference Series*, IOP Publishing, vol. 2108, 2021, p. 012 091.

[12] Y. Jiao and D. Månsson, "Analysis of two hybrid energy storage systems in an off-grid photovoltaic microgrid: A case study," in *2020 IEEE PES Innovative Smart Grid Technologies Europe (ISGT-Europe)*, IEEE, 2020, pp. 554–558.

[13] X. Zhao, Y. W. Li, H. Tian, and X. Wu, "Energy management strategy of multiple supercapacitors in a dc microgrid using adaptive virtual impedance," *IEEE Journal of Emerging and Selected Topics in Power Electronics*, vol. 4, no. 4, pp. 1174–1185, 2016.

[14] *Slideshare, super capacitor*, https://www.slideshare.net/321jestin/super-capacitor, June, 2022.

[15] A. B. Allruwaili, *The impact of different battery technologies for remote microgrids*. South Dakota State University, 2016.

[16] *Save on energy ,tesla powerwall review*, https://www.saveonenergy.com/solar-energy/tesla-powerwall-review/, June, 2022.

[17] *Batteries to be made in australia*, https://www.climatecontrolnews.com.au/renewable-energy/batteries-to-be-made-in-australia, June, 2022.

[18] *Tn power*, https://www.tiannengbatterygroup.com/motive-power-battery/tnet-series/tnet12-125-lead-acid-battery-long-cycle-life. 2022.

[19] *Fire shield , systems limited*, https://www.fireshieldsystemsltd.co.uk/applications/ev-hev/, 2022.

[20] *Pdhsource,flywheel energy storage for area regulation*, https://www.pdhsource.com/product/doe-flywheel-energy-storage-for-are June, 2022.

[21] B. Moran, "Microgrid load management and control strategies," in *2016 IEEE/PES Transmission and Distribution Conference and Exposition (T&D)*, IEEE, 2016, pp. 1–4.

[22] R. Khezri, A. Mahmoudi, and M. H. Khooban, "Microgrids planning for residential electrification in rural areas," in *Residential Microgrids and Rural Electrifications*, Elsevier, 2022, pp. 1–25.

[23] V. Motjoadi, P. N. Bokoro, and M. O. Onibonoje, "A review of microgrid-based approach to rural electrification in south africa: Architecture and policy framework," *Energies*, vol. 13, no. 9, p. 2193, 2020.

[24] H. Pan, M. Ding, A. Chen, R. Bi, L. Sun, and S. Shi, "Research on distributed power capacity and site optimization planning of ac/dc hybrid micrograms considering line factors," *Energies*, vol. 11, no. 8, p. 1930, 2018.

[25] M. S. Mahmoud, *Microgrid: advanced control methods and renewable energy system integration*. Elsevier, 2016.

[26] J. P. Lopes, C. L. Moreira, and A. Madureira, "Defining control strategies for microgrids islanded operation," *IEEE Transactions on power systems*, vol. 21, no. 2, pp. 916–924, 2006.

[27] J. Sahebkar Farkhani, M. Zareein, A. Najafi, R. Melicio, and E. M. Rodrigues, "The power system and microgrid protection—a review," *Applied Sciences*, vol. 10, no. 22, p. 8271, 2020.

[28] H. Haes Alhelou, M. E. Hamedani-Golshan, T. C. Njenda, and P. Siano, "A survey on power system blackout and cascading events: Research motivations and challenges," *Energies*, vol. 12, no. 4, p. 682, 2019.

[29] D. Devaraj, M. K. Paramathma, and I. Rajalakshmi, "Simulation and implementation of phasor measurement unit for wide area monitoring system," in *2017 IEEE International Conference on Intelligent Techniques in Control, Optimization and Signal Processing (INCOS)*, IEEE, 2017, pp. 1–6.

[30] K. E. Martin, G. Benmouyal, M. Adamiak, *et al.*, "Ieee standard for synchrophasors for power systems," *IEEE Transactions on Power Delivery*, vol. 13, no. 1, pp. 73–77, 1998.

[31] A. Ouadi, "Power system protection improvement using wide area synchro-phasor measurements," Ph.D. dissertation, 2015.

[32] L.-A. Lee and V. Centeno, "Comparison of pmu and pmu," in *2018 Clemson University Power Systems Conference (PSC)*, 2018, pp. 1–6. DOI: 10.1109/PSC.2018.8664037.

[33] E. Dusabimana and S.-G. Yoon, "A survey on the micro-phasor measurement unit in distribution networks," *Electronics*, vol. 9, no. 2, p. 305, 2020.

[34] J. Ma, Y. Makarov, and Z. Dong, "Phasor measurement unit and its application in modern power systems," in *Emerging Techniques in Power System Analysis*, Springer, 2010, pp. 147–184.

[35] A. Phadke and J. Thorp, "History and applications of phasor measurements," in *2006 IEEE PES Power Systems Conference and Exposition*, IEEE, 2006, pp. 331–335.

[36] C. Mishra, "Optimal substation coverage for phasor measurement unit installations," Ph.D. dissertation, Virginia Tech, 2012.

[37] W. K. Najy, H. H. Zeineldin, and W. L. Woon, "Optimal protection coordination for microgrids with grid-connected and islanded capability," *IEEE Transactions on industrial electronics*, vol. 60, no. 4, pp. 1668–1677, 2012.

[38] "Ieee standard for synchrophasor measurements for power systems," *IEEE Std C37.118.1-2011 (Revision of IEEE Std C37.118-2005)*, pp. 1–61, 2011. DOI: 10.1109/IEEESTD.2011.6111219.

[39] M. U. Usman and M. O. Faruque, "Applications of synchrophasor technologies in power systems," *Journal of Modern Power Systems and Clean Energy*, vol. 7, no. 2, pp. 211–226, 2019.

[40] M. Meriem, B. Hamid, and O. Abderrahmane, "An investigation of different pmu phasor estimation techniques based on dft using matlab," in *2020 International Conference on Electrical Engineering (ICEE)*, IEEE, 2020, pp. 1–6.

[41] N. M. Tabatabaei, E. Kabalci, and N. Bizon, *Microgrid architectures, control and protection methods*. Springer, 2019.

[42] T. S. Ustun, C. Ozansoy, and A. Zayegh, "Differential protection of microgrids with central protection unit support," in *IEEE 2013 Tencon-Spring*, IEEE, 2013, pp. 15–19.

[43] A. R. Haron, A. Mohamed, H. Shareef, and H. Zayandehroodi, "Analysis and solutions of overcurrent protection issues in a microgrid," in *2012 IEEE International Conference on Power and Energy (PECon)*, IEEE, 2012, pp. 644–649.

[44] G. Asti, S. Kurokawa, E. Costa, and J. Pissolato, "Real-time estimation of transmission line impedance based on modal analysis theory," in *2011 IEEE Power and Energy Society General Meeting*, IEEE, 2011, pp. 1–7.

[45] A. Budner, "Introduction of frequency-dependent line parameters into an electromagnetic transients program," *IEEE Transactions on Power Apparatus and Systems*, no. 1, pp. 88–97, 1970.

[46] J. M. Knezevic and V. A. Katic, "The hybrid method for on-line harmonic analysis," *Advances in Electrical and Computer Engineering*, vol. 11, no. 3, pp. 29–34, 2011.